Postnatal Development of the Hippocampal Formation: A Stereological Study in Macaque Monkeys

Adeline Jabès,[1] Pamela Banta Lavenex,[1] David G. Amaral,[2] and Pierre Lavenex[1]*

[1]Laboratory of Brain and Cognitive Development, Department of Medicine, University of Fribourg, CH-1700 Fribourg, Switzerland
[2]Department of Psychiatry and Behavioral Sciences, Center for Neuroscience, California National Primate Research Center, The M.I.N.D. Institute, University of California Davis, Davis, California 95616

ABSTRACT

We performed a stereological analysis of neuron number, neuronal soma size, and volume of individual regions and layers of the macaque monkey hippocampal formation during early postnatal development. We found a protracted period of neuron addition in the dentate gyrus throughout the first postnatal year and a concomitant late maturation of the granule cell population and individual dentate gyrus layers that extended beyond the first year of life. Although the development of CA3 generally paralleled that of the dentate gyrus, the distal portion of CA3, which receives direct entorhinal cortex projections, matured earlier than the proximal portion of CA3. CA1 matured earlier than the dentate gyrus and CA3. Interestingly, CA1 stratum lacunosum-moleculare, in which direct entorhinal cortex projections terminate, matured earlier than CA1 strata oriens, pyramidale, and radiatum, in which the CA3 projections terminate. The subiculum developed earlier than the dentate gyrus, CA3, and CA1, but not CA2. However, similarly to CA1, the molecular layer of the subiculum, in which the entorhinal cortex projections terminate, was overall more mature in the first postnatal year compared with the stratum pyramidale in which most of the CA1 projections terminate. Unlike other hippocampal fields, volumetric measurements suggested regressive events in the structural maturation of presubicular neurons and circuits. Finally, areal and neuron soma size measurements revealed an early maturation of the parasubiculum. We discuss the functional implications of the differential development of distinct hippocampal circuits for the emergence and maturation of different types of "hippocampus-dependent" memory processes, including spatial and episodic memories. J. Comp. Neurol. 519:1051–1070, 2011.

INDEXING TERMS: hippocampus; neuron number; primate; memory; infantile amnesia; neurodevelopmental disorder

The hippocampal formation comprises a group of cortical regions located in the medial temporal lobe that includes the dentate gyrus, hippocampus, subiculum, presubiculum, parasubiculum, and entorhinal cortex (Amaral and Lavenex, 2007). Although it is well known that damage to the hippocampal formation in adult subjects results in amnesia (Bird and Burgess, 2008; Brown and Aggleton, 2001; Eichenbaum et al., 2007; Morris, 2007; Squire et al., 2007), the precise role of distinct regions of the hippocampal formation in memory function is particularly elusive (Knierim et al., 2006; Poirier et al., 2008; Rolls and Kesner, 2006). In addition, there is a large gap in our understanding of the structural development of the different regions of the primate hippocampal formation and the impact of their maturation on the emergence of particular memory processes (Bauer, 2006; Lavenex et al., 2007a). For example, in the case of developmental amnesia, patients who sustained hippocampal damage early in life exhibit memory impairments affecting preferentially episodic memory (the memory for autobiographical events),

Additional Supporting Information may be found in the online version of this article.

Grant sponsor: Swiss National Science Foundation; Grant number: PP00A-106701; Grant number: PP00P3-124536; Grant number: PMPDP3_122844 (to P.B.L.); Grant number: PMPDP3_128996 (to P.B.L.); Grant sponsor: National Institute of Health; Grant number: RO1-NS16980; Grant number: RR00169 (to the California National Primate Research Center).

*CORRESPONDENCE TO: Dr. Pierre Lavenex, Laboratory of Brain and Cognitive Development, Department of Medicine, University of Fribourg, Chemin du Musée 5, CH-1700 Fribourg, Switzerland.
E-mail: pierre.lavenex@unifr.ch

Received July 10, 2010; Revised August 30, 2010; Accepted November 12, 2010
DOI 10.1002/cne.22549
Published online November 30, 2010 in Wiley Online Library (wileyonlinelibrary.com)

whereas semantic memory (the memory for facts about the world) is largely preserved (Vargha-Khadem et al., 1997). In contrast, lesion of the hippocampus in adults generally impairs both semantic and episodic memory processes (Squire and Zola, 1996). We have recently shown similar functional plasticity in monkeys that received hippocampal lesions early in life. Hippocampal lesions prevented spatial relational learning in adult-lesioned monkeys (Banta Lavenex et al., 2006), whereas spatial relational learning persisted following neonatal lesions (Lavenex et al., 2007b). A systematic quantification of the structural maturation of the primate hippocampal formation would provide fundamental knowledge regarding the development of different functional circuits that might contribute to the emergence and differential maturation of specific declarative memory processes.

All available data indicate that there is significant postnatal maturation of the primate hippocampal formation (Lavenex et al., 2007a; Payne et al., 2010). In the monkey dentate gyrus, for example, although granule cell neuron production decreases considerably during the first few postnatal months, a substantial number of neurons continues to be generated during postnatal development (Eckenhoff and Rakic, 1988; Jabès et al., 2010; Nowakowski and Rakic, 1981; Rakic and Nowakowski, 1981) and adult life (Gould et al., 1999; Jabès et al., 2010; Kornack and Rakic, 1999). Indeed, we have recently shown that about 40% of the total number of granule cells observed in adult (5–9-year-old) macaque monkeys are added to the granule cell layer postnatally (Jabès et al., 2010). Earlier studies also revealed that the dendritic arborization of the granule cells, located in the molecular layer of the dentate gyrus, enlarges substantially during the first 6 postnatal months (Duffy and Rakic, 1983; Seress, 1992). Seress (1992) reported that, at 6 months of age, the appearance and numerical parameters of the entire dendritic tree of individual granule cell neurons are comparable to those of 1-year-old and 3-year-old monkeys. Our own data, however, indicate that the maturation of the dentate granule cell population continues beyond 1 year of age, as the number of mature-sized granule cell neurons is lower in 1-year-old monkeys than in 5–9 year olds (Jabès et al., 2010).

Following the hippocampal circuitry, the targets of the granule cell projections in the polymorphic layer of the dentate gyrus and the CA3 field of the hippocampus also show significant postnatal maturation. Indeed, the morphological characteristics of individual mossy cells in the polymorphic layer (Amaral, 1978; Buckmaster and Amaral, 2001) evolve gradually during at least the first 9 months after birth in monkeys (Seress and Ribak, 1995a) and at least until 30 months after birth in humans (Seress and Mrzljak, 1992). Interestingly, the volume of the polymorphic layer continues to increase after the first 9 postnatal months in monkeys (Jabès et al., 2010), which suggests additional changes in the morphological characteristics of neuronal circuits within this region. The mossy fibers (the axons of the granule cell neurons) also exhibit significant postnatal maturation (Seress and Ribak, 1995b). Indeed, even though the mossy fibers that are already present at birth have mature-appearing synapses and the thorny excrescences present on CA3 pyramidal cells are adult-like, the density of spines on CA3 pyramidal neurons follows a developmental pattern similar to that observed for the mossy cells (Seress and Ribak, 1995a). Moreover, although Timm-stained mossy fiber terminals are visible at birth, overall staining intensity is weaker than that observed in 3-month-old and adult monkeys. The width of CA3 strata pyramidale and lucidum (in which the mossy fibers travel and terminate) reportedly increases further after 6 months of age (see Fig. 4 of Seress and Ribak, 1995b).

Considering the next stage of the hippocampal circuitry, CA1 pyramidal cells are highly differentiated 1 month before birth (Khazipov et al., 2001). However, comparison of the morphological characteristics of prenatal CA1 pyramidal cells (Khazipov et al., 2001) with those of postnatal and adult monkey CA1 pyramidal cells (Altemus et al., 2005) suggests that further growth and remodeling of the dendritic arborization continues after birth. This is in agreement with preliminary data reported by Seress (2001) suggesting changes in spine density and myelin formation up to the seventh postnatal month in CA1 in monkeys. Similarly, in humans, although CA1 pyramidal cells exhibit early morphological differentiation and calbindin immunoreactivity (Abraham et al., 2009), myelination might continue beyond 8 years of age in stratum radiatum of CA1 (Abraham et al., 2010).

There is very little information regarding the postnatal development of the other hippocampal regions in primates. We previously reported preliminary data based on the immunohistochemical detection of nonphosphorylated high-molecular-weight neurofilaments (Lavenex et al., 2004). In 3-week-old monkeys, only the subiculum exhibited significant immunostaining, and the processes that were labeled in infants were relatively fewer and less intensely labeled compared with adults. In contrast, staining was near background levels in CA3 of both 3-week-old and 3-month-old monkeys. CA2 exhibited moderate staining at 3 months but not at 3 weeks of age. To our knowledge, there are no study has described the structural postnatal maturation of the primate presubiculum or parasubiculum. All the available data, therefore, derive from miscellaneous studies using different methodologies at various developmental stages. Notably absent is a systematic, quantitative evaluation of the postnatal

structural development of individual regions of the primate hippocampal formation.

For this study, we used stereological techniques to characterize and quantify the morphological changes underlying the structural maturation of the dentate gyrus; CA3, CA2, and CA1 fields of the hippocampus; subiculum; presubiculum; and parasubiculum in macaque monkeys during early postnatal development. The analysis of the entorhinal cortex will be the subject of a future, separate study.

MATERIALS AND METHODS

Animals and tissue processing

Brain acquisition

Twenty-four rhesus monkeys, *Macaca mulatta*, four 1-day-olds (2 M, 2 F), four 3-month-olds (2 M, 2 F), four 6-month-olds (2 M, 2 F), four 9-month-olds (2 M, 2 F), four 1-year-olds (2 M, 2 F), and four adults [5.3, 9.4 (M), 7.7 and 9.3 (F) years of age] were used for this study. Monkeys were born from multiparous mothers and raised at the California National Primate Research Center (CNPRC). They were maternally reared in 2,000-m^2 outdoor enclosures and lived in large social groups until they were killed. These animals were the same animals used in a previous study on postnatal neurogenesis and neuron number in the dentate gyrus (Jabès et al., 2010). All experimental procedures were approved by the Institutional Animal Care and Use Committee of the University of California, Davis, and were in accordance with the National Institutes of Health guidelines for the use of animals in research.

Monkeys were deeply anesthetized with an intravenous injection of sodium pentobarbital (50 mg/kg i.v.; Fatal-Plus; Vortech Pharmaceuticals, Dearborn, MI) and perfused transcardially with 1% and then 4% paraformaldehyde in 0.1 M phosphate buffer (PB; pH 7.4) following protocols previously described (Banta Lavenex et al., 2006; Lavenex et al., 2009a). Coronal sections were cut with a freezing microtome into six 30-μm series and one series at 60 μm (Microm HM 450). The 60-μm sections were collected in 10% formaldehyde solution in 0.1 M PB (pH 7.4) and postfixed at 4°C for 4 weeks prior to Nissl staining with thionin. All other series were collected in tissue collection solution (TCS) and kept at −70°C until further processing.

Nissl staining

The procedure for Nissl-stained sections followed our standard laboratory protocol described previously (Lavenex et al., 2009a). Sections were taken out of the 10% formaldehyde solution, thoroughly washed for 2 × 2 hours in 0.1 M PB (pH 7.4), mounted on gelatin-coated slides from filtered 0.05 M phosphate buffer (pH 7.4), and air dried overnight at 37°C. Sections were then defatted for 2 × 2 hours in a mixture of chloroform/ethanol (1:1, vol.) and rinsed for 2 × 2 minutes in 100% ethanol, 1 × 2 minutes in 95% ethanol, and air dried overnight at 37°C. Sections were then rehydrated through a graded series of ethanol, 2 minutes in 95% ethanol, 2 minutes in 70% ethanol, 2 minutes in 50% ethanol; dipped in two separate baths of dH_2O; and stained for 20 seconds in a 0.25% thionin (Fisher Scientific, Waltham, MA; catalog No. T-409) solution, then dipped in two separate baths of dH_2O, 4 minutes in 50% ethanol, 4 minutes in 70% ethanol, 4 minutes in 95% ethanol + glacial acetic acid (1 drop per 100 ml of ethanol), 4 minutes in 95% ethanol, 2 × 4 minutes in 100% ethanol, 3 × 4 minutes in xylene; and coverslipped with DPX (BDH Laboratories, Poole, United Kingdom).

SMI-32 immunohistochemistry

The immunohistochemical procedure for visualizing nonphosphorylated high-molecular-weight neurofilaments was carried out on free-floating sections using the monoclonal antibody SMI-32 (Alexis Biochemicals, Lausen, Switzerland; catalog No. CO-SMI-32R-0500), as previously described (Lavenex et al., 2009a). This antibody was raised in mouse against the nonphosphorylated 200-kDa heavy neurofilament. On conventional immunoblots, SMI-32 visualizes two bands (200 and 180 kDa), which merge into a single NFH line on two-dimensional blots (Goldstein et al., 1987; Sternberger and Sternberger, 1983). This antibody has been shown to react with nonphosphorylated high-molecular-weight neurofilaments of most mammalian species, including rats, cats, dogs, monkeys, and humans (de Haas Ratzliff and Soltesz, 2000; Hof and Morrison, 1995; Hornung and Riederer, 1999; Lavenex et al., 2004; Siegel et al., 1993) and may also show some limited cross-reactivity with nonphosphorylated medium-molecular-weight neurofilaments (Hornung and Riederer, 1999).

Stereological analyses

Neuron number

The total number of neurons in the principal layers of the dentate gyrus (granule cell layer), CA3, CA2, CA1, subiculum (pyramidal cell layer), presubiculum, and parasubiculum (layer II) was determined using the optical fractionator method on the Nissl-stained sections cut at 60 μm (Lavenex et al., 2000a,b; West et al., 1991). This design-based method allows estimation of the number of neurons that is independent of volume estimates (Lavenex et al., 2000b). About 30 sections per animal (480 μm apart), with the first section selected randomly within the first two sections through the dentate gyrus and the last section included based on the presence of a clearly identifiable granule cell layer, were used for the estimation of the total number of principal neurons in the different

regions of the hippocampal formation. We chose to leave out the most rostral and caudal portions of certain fields in order to avoid a biased sampling resulting from the tangential cut of these extreme regions in coronal sections. We used a ×100 Plan Fluor oil objective (N.A. 1.30) on a Nikon Eclipse 80i microscope (Nikon Instruments Inc, Melville, NY) linked to PC-based StereoInvestigator 7.0 (MicroBrightField, Williston, VT). The sampling scheme for each region is presented as Supporting Information; sampling schemes were established to obtain individual estimates of neuron number with coefficients of error (CE) lower than 0.10.

Neuronal soma size

The volume of the soma of principal neurons within the dentate gyrus, CA3, CA2, CA1, subiculum, presubiculum, and parasubiculum was determined using the nucleator method on Nissl-stained sections (Gundersen, 1988; Lavenex, 2009; Lavenex et al., 2009a). Briefly, the nucleator can be used to estimate the mean cross-sectional area and volume of cells. A set of rays emanating from a randomly chosen point within the nucleus or nucleolus is drawn and oriented randomly. The length of the intercept from the point to the cell boundary (l) is measured, and the cell volume is obtained by $V = (4/3 \cdot 3.1416) \cdot l^3$. Essentially, this is the formula used to determine the volume of a sphere with a known radius. Note that the nucleator method provides accurate estimates of neuron size when isotropic-uniform-random sectioning of brain structures is employed (Gundersen, 1988). In our study, all brains were cut in the coronal plane. Estimates of cell size might therefore be impacted by the nonrandom orientation of neurons in the different structures of the monkey hippocampal formation, which could lead to a systematic over- or underestimation of cell size in any given structure. However, this methodological limitation does not impact the conclusions of the current study, because the brains from different age groups were processed and analyzed in the same manner.

In the dentate gyrus, 200–400 neurons per animal chosen randomly during the optical fractionator analysis of neuron number were measured. In CA3, 250–400 neurons per animal chosen randomly during the optical fractionator analysis were measured. In CA2, CA1, subiculum, presubiculum, and parasubiculum, all neurons counted during the optical fractionator analysis were measured (CA2: 130–330; CA1: 150–400; subiculum: 170–370; presubiculum: 200–500; parasubiculum: 200–400).

Volume of distinct regions and individual layers

The volume of the different layers of distinct hippocampal regions was measured according to the Cavalieri principle on Nissl-stained sections cut at 60 μm (Gundersen and Jensen, 1987; Lavenex et al., 2000a,b; West and Gundersen, 1990). We used a ×4 Plan Fluor objective (N.A. 0.13) on a Nikon Eclipse 80i microscope linked to PC-based StereoInvestigator 7.0. About 30 sections per animal (480 μm apart) were used for the measurements of the dentate gyrus layers. About 15 sections per animal (960 μm apart) were used for the measurements of the different layers of CA3, CA2, CA1, subiculum, and presubiculum; the same number of sections, 480 μm apart, was used for the parasubiculum. The first section was selected randomly within the first two sections through the dentate gyrus. As for the determination of neuron number, we chose to leave out the most rostral and caudal portions of certain fields in order to avoid a biased sampling resulting from the tangential cut of these extreme regions in coronal sections.

In contrast to the estimates of neuron number, estimates of the volume of distinct regions and individual layers, as well as neuronal soma size, might potentially be impacted by the differential shrinkage of brain tissue upon perfusion and fixation at different ages across postnatal development. Indeed, postprocessing section thickness was less in newborns compared with other ages (Supp. Info.). However, the results presented below reveal a differential volumetric development of distinct hippocampal regions and individual layers that cannot be accounted for by overall age-specific differences in brain tissue shrinkage. Moreover, a number of parameters, including neuronal soma size and volume of individual layers, did not reveal any differences between ages, arguing against a general confound resulting from differential shrinkage across development.

Statistical analyses

We performed ANOVAs with age as a factor to analyze volume and neuron number measurements. Post hoc analyses were performed with the Fisher PLSD test. We also performed two-way repeated-measures ANOVAs, with age as a factor and regions or layers as repeated measures, to compare the relative growth of distinct hippocampal regions or individual layers in the first year after birth. The significance level was set at $P < 0.05$ for all analyses.

Statistical analyses of soma size were performed on the modes for the dentate gyrus, because the distribution of granule cell size was bimodal across ages. For all the other structures, statistical analyses were performed on the average soma size for each individual, because soma size was normally distributed.

No gender differences were found for any of the measured parameters, so data from both genders were combined for presentation. We also evaluated each structure

in a systematic manner on the left or right side: we measured the left hippocampal formation for one male and one female, and the right hippocampal formation for one male and one female, in each age group. No lateralization was found for any of the measured parameters. Thus, our findings and all subsequent considerations are valid and can be generalized to both the left and the right hippocampal formation in males and females. All sections used in this study were coded to allow blind analysis, and the code was broken only after completion of the analyses.

Photomicrograph production

Photomicrographs were taken with a Leica DFC490 digital camera (Leica Microsystems, Wetzlar, Germany) on a Nikon Eclipse 80i microscope (Nikon Instruments, Tokyo, Japan). Artifacts located outside the sections were removed, and levels were adjusted in Adobe Photoshop CS, version 8.0 (Adobe, San Jose, CA).

RESULTS

Structural organization of the monkey hippocampal formation

The nomenclature and cytoarchitectonic subdivisions of the monkey hippocampal formation have been described in detail previously (Amaral et al., 1984; Amaral and Lavenex, 2007; Pitkanen and Amaral, 1993). We provide here a summary of the main morphological characteristics of each region observed in coronal Nissl-stained sections, which were used to determine the boundaries of individual regions in rhesus monkeys (*Macaca mulatta*; Fig. 1). We also provide additional descriptions based on the patterns of SMI-32 immunoreactivity, which provide useful indications for the definition of certain borders that might be difficult to identify in Nissl-stained sections. We focused our stereological analyses on the dentate gyrus; the CA3, CA2, and CA1 fields of the hippocampus; subiculum; presubiculum; and parasubiculum. As mentioned above, the analysis of the entorhinal cortex will be the subject of a future, separate report.

The dentate gyrus comprises three layers: the principal cell layer, a densely packed granule cell layer; a relatively cell-free molecular layer that lies superficial to the granule cell layer and ends at the hippocampal fissure or ventricle; and a rather narrow, polymorphic layer located subjacent to the granule cell layer, which harbors a variety of neuronal cell types (Amaral and Lavenex, 2007; Amaral et al., 2007; Lavenex and Amaral, 2000; Lavenex et al., 2009a). We delineate these three layers according to these descriptions for all subsequent analyses. Note that a detailed analysis of postnatal neurogenesis and neuron number in the monkey dentate gyrus has been published previously (Jabès et al., 2010). We report some of these findings here in order to provide a complete description of the differential maturation of individual regions and layers of the monkey hippocampal formation during early postnatal life.

The hippocampus is divided into three distinct fields, CA3, CA2 and CA1. CA3 and CA2 are characterized by large pyramidal cells, which are located in a relatively compact principal cell layer. The proximal part of CA3 occupies much of the region enclosed within the limbs of the dentate gyrus. The distal part of CA3 appears more compact and darkly stained in Nissl-stained sections than the proximal part. CA2 is differentiated from CA3 by the lack of a mossy fiber input (i.e., projections from the dentate gyrus granule cells; Kondo et al., 2008). CA1 has smaller and more spherical pyramidal cells in its principal cell layer, which is substantially thicker and less densely packed than in CA3 and CA2. The widening of the pyramidal cell layer in CA1 therefore marks the border between CA2 and CA1. Although SMI-32 immunoreactivity varies during postnatal development, SMI-32 staining provides useful landmarks to delineate these three fields. Indeed, CA1 is not stained at any age, whereas CA2 is already lightly stained at birth and is darkly stained at 3 months of age. Similarly, the proximal part of CA3 is not stained during early postnatal development and is moderately stained in adulthood, whereas the distal part of CA3 is moderately stained during early postnatal development and is darkly stained in adulthood (Lavenex et al., 2004).

The hippocampus is also subdivided into a number of laminae that run parallel to the pyramidal cell layer. Subjacent to the pyramidal cell layer is the cell-poor stratum oriens, which in CA1 is less apparent and not clearly identifiable because of the widening and decreased density of the pyramidal cell layer. Stratum oriens can be defined as the infrapyramidal region in which some of the CA3-to-CA3 associational connections and the CA3-to-CA1 Schaffer collateral connections are located. In rats, stratum oriens contains the basal dendrites of the densely packed pyramidal cells, whereas, in monkeys, the basal dendrites of the pyramidal cells are also largely located in the loosely packed pyramidal cell layer (Altemus et al., 2005). We therefore included stratum oriens with the pyramidal cell layer in the volumetric measurements in all fields. Deep to stratum oriens is the thin, fiber-containing alveus. Superficial to the pyramidal cell layer in CA3 is stratum lucidum, in which some of the mossy fibers travel. The distal part of stratum lucidum, called the end bulb, thickens where the mossy fibers bend rostrally and travel longitudinally for 3–5 mm or about 30% of the length of the hippocampus (Kondo et al., 2008); the end bulb helps to delineate the border between CA3 and CA2. Unlike the rat, in which most mossy fibers travel in a position just superficial to the pyramidal cell layer, mossy

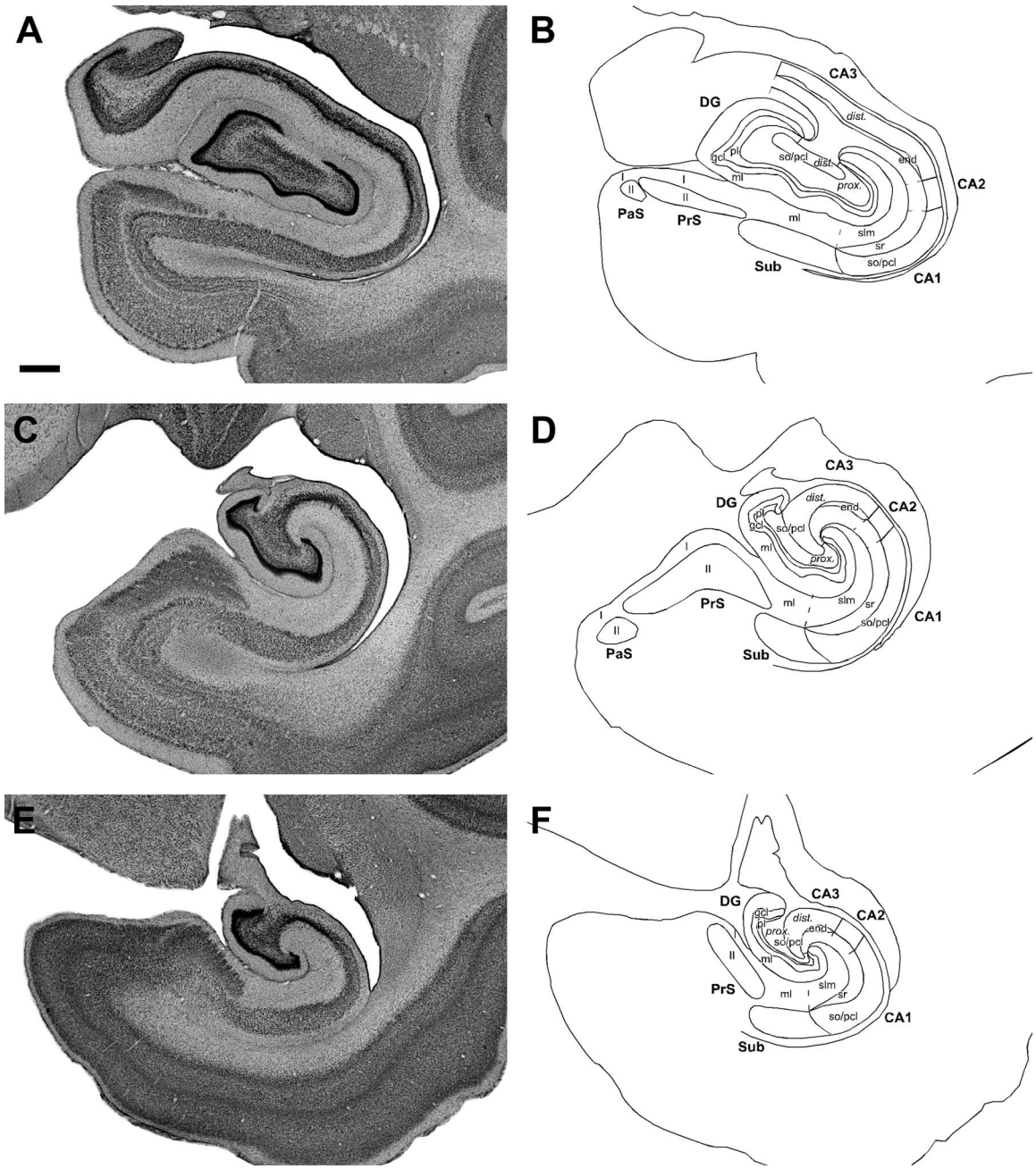

Figure 1. *A–F*: Coronal, Nissl-stained sections (A,C,E) and corresponding line drawings (B,D,F) at three different rostrocaudal levels of the newborn rhesus monkey hippocampal formation. **G–L**: Coronal, Nissl-stained sections (G,I,K) and corresponding line drawings (H,J,L) at similar rostrocaudal levels of the adult rhesus monkey hippocampal formation. Line drawings delineate the different hippocampal fields and layers measured in this study. DG, dentate gyrus; ml, molecular layer; gcl, granule cell layer; pl, polymorphic layer; CA3, CA2, CA1, fields of the hippocampus proper; CA3prox, proximal portion of CA3; CA3dist, distal portion of CA3; so, stratum oriens; pcl, pyramidal cell layer; sl, stratum lucidum; end, end bulb; sr, stratum radiatum; slm, stratum lacunosum-moleculare; Sub, subiculum; PrS, presubiculum; PaS, parasubiculum; EC, entorhinal cortex. Scale bars = 1 mm.

fibers travel both within and above the pyramidal cell layer throughout the entire CA3 in monkeys (Kondo et al., 2008). Stratum radiatum is located superficial to stratum lucidum in CA3 and immediately above the pyramidal cell layer in CA2 and CA1. Stratum radiatum can be defined as the suprapyramidal region in which the CA3-to-CA3 associational connections and the CA3-to-CA1 Schaffer collateral connections are located (Kondo et al., 2009). The most superficial layer of the hippocampus is called stratum lacunosum-moleculare. It is in this layer that fibers from the entorhinal cortex terminate (Witter and Amaral, 1991).

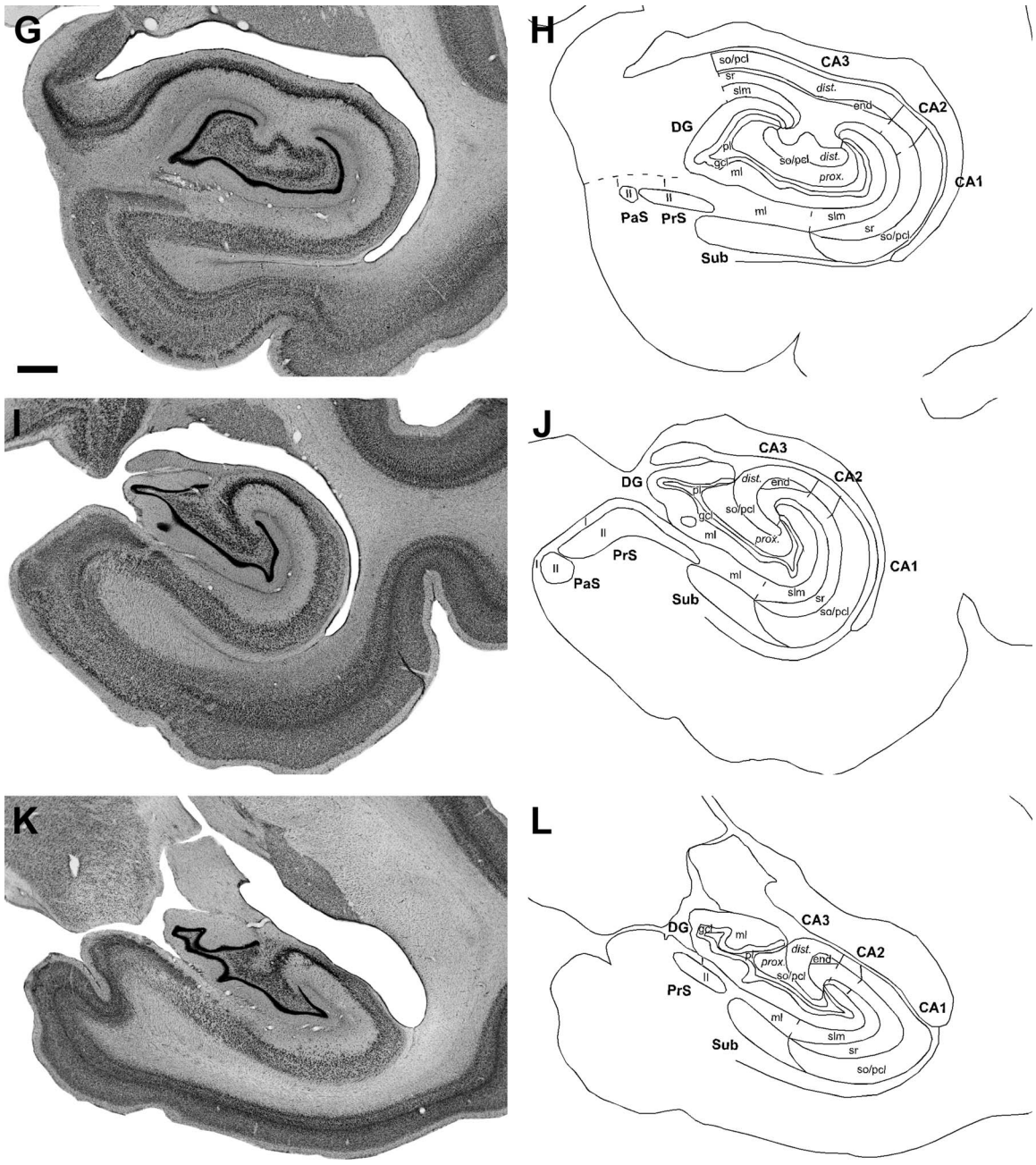

Figure 1. (*Continued*)

The border of CA1 with the subiculum is oblique; the progressively thinner CA1 pyramidal cell layer actually extends over the initial portion of the subiculum (Fig. 1). The pyramidal cell layer of the subiculum is slightly broader than that of CA1. The cell population in the subiculum pyramidal cell layer is more heterogeneous than in CA1, and the orientation is slightly different. CA1 stratum radiatum ends at the superficial CA1/subiculum border, and the relatively cell-free zone superficial to the pyramidal cell layer in the subiculum is called the molecular layer. A relatively high level of SMI-32 immunoreactivity, particularly in the proximal segments of apical dendrites, distinguishes the subiculum from both CA1 and presubiculum throughout postnatal development.

The presubiculum lies medial to the subiculum. It consists of a cell-free layer I and a densely packed, superficial layer II composed of small pyramidal cells. At caudal levels, this superficial cell layer is further subdivided and includes a thin band of larger and more darkly stained neurons near its superficial margin. There is a second, deep layer of cells in the presubiculum, but it is not clear whether this layer should be considered part of the

TABLE 1.

Number of Principal Neurons (in Thousands ± SEM) in the Macaque Monkey Hippocampal Formation[1]

	Birth	3 Months	6 Months	9 Months	1 Year	5–9 Years	Average
Dentate gyrus	4,392 ± 206	6,129 ± 360	6,347 ± 283	6,528 ± 479	6,994 ± 471	7,213 ± 257	–
CA3 total	933 ± 38	988 ± 69	937 ± 50	988 ± 50	991 ± 28	868 ± 32	951 ± 19
Proximal	325 ± 23	354 ± 28	350 ± 33	366 ± 25	414 ± 28	337 ± 17	358 ± 11
Distal	608 ± 25	634 ± 51	587 ± 34	622 ± 50	577 ± 33	530 ± 19	593 ± 15
CA2	112 ± 6	121 ± 2	118 ± 5	123 ± 9	124 ± 8	106 ± 6	117 ± 3
CA1	1,015 ± 31	977 ± 52	1,056 ± 50	1,036 ± 44	1,056 ± 57	888 ± 8	1,005 ± 20
Subiculum	518 ± 26	476 ± 22	463 ± 23	460 ± 25	473 ± 28	447 ± 11	473 ± 10
Presubiculum	1,578 ± 91	1,457 ± 66	1,473 ± 30	1,520 ± 111	1,420 ± 85	1,255 ± 52	1,450 ± 35
Parasubiculum	223 ± 10	217 ± 10	203 ± 6	222 ± 19	197 ± 8	206 ± 2	211 ± 4

[1]N = 4 per age (2 males, 2 females); average across ages: n = 24 individuals (12 males, 12 females). Note that an average value was calculated only when there was no statistical difference between age groups.

presubiculum or part of the adjoining parasubiculum. There is, however, some evidence from connectional studies suggesting that this layer is more closely related to the deeper layers of the medial entorhinal cortex (Amaral et al., 1984). Accordingly, we did not consider this deep layer as part of the presubiculum. Moderate SMI-32 immunoreactivity distinguishes the presubiculum from the darkly stained subiculum and the unstained parasubiculum throughout postnatal development.

The cytoarchitectonic organization of the parasubiculum is quite variable along its rostrocaudal extent, and its cell population is heterogeneous. The parasubiculum comprises two layers: a cell-free layer I and a densely packed cell layer II. Layer II is usually fairly well demarcated from both the presubiculum and the entorhinal cortex by two narrow, cell-poor zones on either side of it (Amaral et al., 1984). In contrast, the cell layers deep to layer II are indistinguishable from the deep layers of the entorhinal cortex (Bakst and Amaral, 1984). Accordingly, we did not consider these deep layers as part of the parasubiculum.

Stereological findings

Even a cursory examination of Nissl-stained coronal brain sections is sufficient to demonstrate that the monkey hippocampal formation is not mature at birth (Fig. 1). Here, we performed a systematic, stereological study to provide quantitative data on neuron number, neuronal soma size, and neuropil volume in the hippocampal formation of developing monkeys from birth to 1 year of age and in sexually mature monkeys between 5 and 9 years of age. These data provide fundamental information regarding the differential, structural maturation of distinct regions, layers, and putative functional circuits in the monkey hippocampal formation during early postnatal life.

Neuron number

The numbers of principal neurons found in the different regions of the monkey hippocampal formation are presented in Table 1. As reported previously (Jabès et al., 2010), the number of neurons found in the granule cell layer of the dentate gyrus, one of two brain regions where significant neurogenesis occurs postnatally, differed between age groups ($F_{5,18} = 7.844$, $P < 0.001$). There was a large difference in neuron number between newborn (4.39 ± 0.21 million) and 3-month-old monkeys (6.13 ± 0.36 million; $P = 0.003$). After 3 months of age, neuron number increased further to reach 7.21 ± 0.26 million granule cells in 5–9-year-old monkeys. These data therefore revealed that about 40% of the total number of neurons found in the granule cell layer of 5–9-year-old monkeys are added postnatally, with a peak of neuron addition (25%) during the first 3 months after birth.

As expected, we found no differences in neuron number between age groups in the other regions of the hippocampal formation, where neurogenesis has not been observed postnatally (Table 1; CA3 proximal, $F_{5,18} = 1.422$, $P = 0.264$; CA3 distal, $F_{5,18} = 0.999$, $P = 0.446$; CA2, $F_{5,18} = 1.327$, $P = 0.297$; CA1, $F_{5,18} = 2.159$, $P = 0.105$; subiculum, $F_{5,18} = 1.123$, $P = 0.383$; presubiculum, $F_{5,18} = 2.038$, $P = 0.122$; and parasubiculum, $F_{5,18} = 1.068$, $P = 0.410$). Altogether, our quantitative data established that 40% of the granule cell neurons found in the mature dentate gyrus are added postnatally, whereas the total number of principal neurons found in the other regions of the monkey hippocampal formation is stable from birth to young adulthood (5–9 years of age).

Neuron size

We also measured the volume of neuronal somas in order to characterize the structural maturation of the principal neurons in the different regions of the monkey hippocampal formation throughout postnatal development (Table 2; see also Supp. Info. for illustrations of the distributions of neuronal soma size at different ages). In the granule cell layer of the dentate gyrus, neuronal soma size exhibited a bimodal distribution across ages (mode 1: <150 μm^3; mode 2: 400–550 μm^3): a large population

TABLE 2.

Soma Size (μm^3 ± SEM) of Principal Neurons in the Macaque Monkey Hippocampal Formation[1]

	Birth	3 Months	6 Months	9 Months	1 Year	5–9 Years	Average
Dentate gyrus	578 ± 25	542 ± 37	536 ± 24	553 ± 24	503 ± 12	544 ± 46	543 ± 12
CA3 total	2,914 ± 159	3,004 ± 245	3,132 ± 206	3,432 ± 176	3,095 ± 82	3,516 ± 154	–
Proximal	2,255 ± 86	2,648 ± 227	3,014 ± 250	3,314 ± 130	2,892 ± 93	3,496 ± 188	–
Distal	3,295 ± 200	3,234 ± 260	3,193 ±192	3,503 ± 221	3,256 ± 80	3,532 ± 168	3,335 ± 76
CA2	2,673 ± 90	2,401 ± 248	2,750 ± 190	2,448 ± 389	2,573 ±294	2,465 ± 217	2,552 ± 96
CA1	2,129 ± 163	2,184 ± 207	2,684 ± 173	2,625 ± 383	2,565 ± 313	2,783 ± 282	2,495 ± 109
Subiculum	2,038 ± 92	1,890 ± 196	2,191 ± 153	2,121 ± 229	1,958 ± 243	1,861 ± 174	2,010 ± 72
Presubiculum	1,015 ± 55	1,070 ± 66	1,010 ± 29	1,072 ± 51	922 ± 28	754 ± 22	–
Parasubiculum	1,283 ± 56	1,255 ± 66	1,273 ± 39	1,305 ± 37	1,243 ± 44	1,249 ± 46	1,268 ± 18

[1]N = 4 per age (2 males, 2 females); average across ages: n = 24 individuals (12 males, 12 females). Note that an average value was calculated only when there was no statistical difference between age groups.

of small cells most prominent during the first months after birth gradually gave way to mature-sized cells (Supp. Info.). Accordingly, the number of small cells differed between age groups ($F_{5,18} = 5.183$, $P = 0.004$). After a transient increase in the number of small cells between birth and 3 months of age ($P = 0.016$), which corresponds to the peak of neuronal addition (Jabès et al., 2010), the small cell population decreased gradually within the first year after birth. Interestingly, the number of small cells was still significantly higher in 1-year-old monkeys compared with 5–9-year-old monkeys ($P = 0.023$). Similarly, the number of mature-sized cells differed between age groups ($F_{5,18} = 14.582$, $P < 0.001$). The mature-sized cell population exhibited a gradual increase between birth and 1 year of age (newborn < 6 months, 9 months, and 1 year, all $P < 0.05$; 3 months <1 year, $P = 0.005$), and, most importantly, the number of mature-sized cells was lower in 1-year-old monkeys compared with 5–9 year olds ($P = 0.022$). These data indicate that monkey granule cell neurons undergo a gradual but substantial structural maturation from birth until beyond the first year after birth in order to achieve mature morphological characteristics.

In the other hippocampal regions with stable neuron numbers after birth, some principal neuron populations exhibited significant morphological changes during early postnatal development (Table 2; Supp. Info.). Indeed, in the proximal portion of CA3 (enclosed within the blades of the dentate gyrus; Fig. 1), the average neuronal soma size increased during postnatal development ($F_{5,18} = 6.649$, $P = 0.001$; Supp. Info.). Neuronal soma size increased most significantly during the first 3 months after birth (newborn < 6 months, 9 months, 1 year, and 5–9 years, all $P < 0.05$; 3 months < 5–9 years, $P = 0.022$). In the presubiculum, the average neuronal soma size differed among age groups ($F_{5,18} = 7.274$, $P < 0.001$; Supp. Info.). Surprisingly, neuronal soma size appeared to decrease between 1 year and 5–9 years of age (5–9 years < all other ages, $P < 0.05$).

In contrast, we found no significant changes in neuronal soma size during postnatal development in any other region of the monkey hippocampal formation (Table 2; Supp. Info.): distal portion of CA3 ($F_{5,18} = 0.553$, $P = 0.734$), CA2 ($F_{5,18} = 0.293$, $P = 0.911$), CA1 ($F_{5,18} = 1.051$, $P = 0.419$), subiculum ($F_{5,18} = 0.481$, $P = 0.786$), parasubiculum ($F_{5,18} = 0.234$, $P = 0.942$).

In sum, our quantitative data revealed a protracted development of the dentate gyrus granule cell population, which continues beyond the first year after birth and therefore extends well past the period of major neuron production. Interestingly, neuronal soma size in the proximal part of CA3, which receives a strong projection from the dentate gyrus granule cells but no direct entorhinal cortex input (Kondo et al., 2008; Witter and Amaral, 1991), increased the most within the first 3 postnatal months at the peak of neuron addition in the dentate gyrus. In contrast, neuronal soma size did not increase in the other regions of the monkey hippocampal formation during postnatal development.

Volumetric development of distinct hippocampal regions

A major characteristic of the hippocampal formation is the clear regional and laminar organization of its functional circuits (Fig. 2; Amaral and Lavenex, 2007). We therefore performed regional volume measurements to evaluate the structural maturation of distinct hippocampal regions (Table 3). We further compared the percentage of the adult volume of individual hippocampal regions (dentate gyrus, CA3, CA2, CA1, and subiculum) at birth, 3 months, 6 months, 9 months, and 1 year of age (Fig. 3). We found that, although the volume of most regions differed between newborn and 1-year-old monkeys (age: $F_{4,60} = 8.709$, $P < 0.001$), some regions exhibited greater volumetric differences and were relatively more developed than others within the first year after birth (regions: $F_{4,60} = 21.179$, $P < 0.001$; interaction: $F_{16,60} = 1.797$, $P = 0.053$). Indeed, the dentate gyrus and CA3 were overall less well developed than CA2, CA1, and

subiculum in the first year of life (DG < CA2 = CA1 = Sub, $P < 0.001$; CA3 < CA2 = CA1 = Sub, $P < 0.001$; DG < CA3, $P < 0.05$).

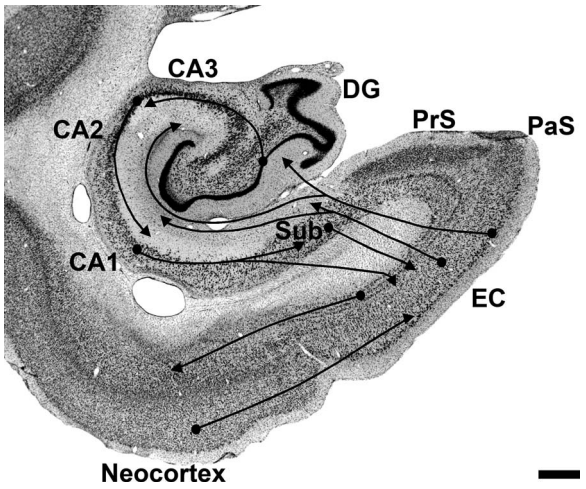

Figure 2. Schematic representation of the hierarchical organization of the main serial and parallel pathways through the different regions of the monkey hippocampal formation. EC, entorhinal cortex; DG, dentate gyrus; CA3, CA2, CA1, fields of the hippocampus; Sub, subiculum; PrS, presubiculum; PaS, parasubiculum. Scale bar = 1 mm.

CA2 and the subiculum were volumetrically more mature than the DG, CA3, and CA1 at birth (all $P < 0.05$). At 6 months of age, however, CA1 had attained a level of maturation similar to that of CA2 and the subiculum (both $P > 0.05$). At 1 year of age, the dentate gyrus and CA3 were less well developed volumetrically than CA1 (both $P < 0.05$). Altogether, these volumetric data reveal a differential maturation of distinct regions of the monkey hippocampal formation during the first year after birth.

Volumetric development of distinct layers within each region

We performed laminar volume measurements in the different hippocampal regions in order to describe further their postnatal maturation and characterize the structural maturation of putative functional circuits (Fig. 2; Amaral and Lavenex, 2007). We present the quantitative data on individual layers in Table 3.

Dentate gyrus

The volume of the granule cell layer differed between age groups ($F_{5,18} = 5.718$, $P = 0.002$). In newborn monkeys, the volume of the granule cell layer was about 60% of that observed in 5–9-year-old monkeys; in 1-year-olds, it was 88% of the volume observed in 5–9-year-olds. The

TABLE 3.
Volume of Individual Layers (mm^3 ± SEM) in Distinct Hippocampal Regions of Macaque Monkeys[1]

	Birth	3 Months	6 Months	9 Months	1 Year	5–9 Years	Average
Dentate gyrus total	31.9 ± 2.7	42.5 ± 4.7	45.5 ± 2.6	50.6 ± 2.8	56.6 ± 2.5	66.7 ± 3.5	–
gcl	6.4 ± 0.6	7.7 ± 0.9	8.1 ± 0.6	9.0 ± 0.5	9.5 ± 0.5	10.8 ± 0.6	–
ml	20.0 ± 1.6	28.8 ± 3.2	31.3 ± 1.8	35.0 ± 2.0	39.4 ± 1.6	46.2 ± 2.5	–
pl	5.5 ± 0.6	6.0 ± 0.7	6.1 ± 0.3	6.6 ± 0.3	7.7 ± 0.4	9.7 ± 0.4	–
CA3 total	30.3 ± 2.5	35.6 ± 3.2	38.7 ± 2.0	41.8 ± 3.6	44.6 ± 2.7	51.9 ± 2.8	–
so/pcl proximal	5.5 ± 0.6	8.4 ± 0.9	9.3 ± 1.2	10.9 ± 1.1	12.3 ± 1.6	15.6 ± 1.5	–
so/pcl distal	16.9 ± 1.8	17.9 ± 1.4	18.4 ± 0.7	20.2 ± 2.1	20.3 ± 1.3	22.9 ± 1.1	19.4 ± 0.7
endbulb	1.3 ± 0.1	2.3 ± 0.2	2.2 ± 0.3	2.1± 0.2	3.0 ± 0.3	3.1 ± 0.5	–
sr	4.5 ± 0.4	4.9 ± 0.7	6.2 ± 0.5	6.4 ± 0.9	6.1 ± 0.5	7.2 ± 0.3	–
slm	2.2 ± 0.4	2.1 ± 0.4	2.5 ± 0.3	2.2 ± 0.1	2.9 ± 0.1	3.1 ± 0.4	2.5 ± 0.1
CA2 total	6.0 ± 0.2	6.1 ± 0.1	6.2 ± 0.4	6.4 ± 0.4	6.8 ± 0.4	7.1 ± 0.4	6.4 ± 0.1
so/pcl	2.5 ± 0.2	2.6 ± 0.1	2.3 ± 0.2	2.4 ± 0.2	2.7 ± 0.1	2.9 ± 0.2	2.6 ± 0.1
sr	1.9 ± 0.2	2.2 ± 0.01	2.4 ± 0.2	2.5 ± 0.2	2.5 ± 0.2	2.7 ± 0.2	2.4 ± 0.1
slm	1.6 ± 0.1	1.4 ± 0.1	1.5 ± 0.05	1.5 ± 0.1	1.6 ± 0.1	1.5 ± 0.1	1.5 ± 0.04
CA1 total	41.7 ± 4.1	60.0 ± 6.0	70.2 ± 3.7	70.9 ± 2.9	76.0 ± 3.1	75.3 ± 3.7	–
so/pcl	20.5 ± 2.2	30.7 ± 3.0	36.4 ± 1.4	36.7 ± 1.4	38.7 ± 1.7	40.8 ± 1.7	–
sr	9.5 ± 1.0	14.2 ± 1.3	17.6 ± 1.1	18.9 ± 1.8	19.6 ± 0.9	18.8 ± 1.4	–
slm	11.8 ± 0.9	15.1 ± 1.9	16.3 ± 1.5	15.3 ± 0.7	17.8 ± 0.7	15.6 ± 1.4	15.3 ± 0.6
Subiculum total	21.7 ± 1.9	24.0 ± 2.3	26.1 ± 1.9	27.7 ± 2.1	27.0 ± 0.4	29.2 ± 1.2	25.9 ± 0.8
pcl	12.9 ± 1.3	14.8 ± 1.3	15.6 ± 0.8	16.4 ± 1.3	16.2 ± 0.3	18.1 ± 0.8	–
ml	8.8 ± 0.7	9.1 ± 1.0	10.5 ± 1.2	11.3 ± 0.8	10.8 ± 0.6	11.1 ± 0.6	10.3 ± 0.4
Presubiculum total	23.7 ± 1.7	23.4 ± 1.6	21.5 ± 1.1	21.9 ± 1.1	22.5 ± 1.1	19.0 ± 1.4	22.0 ± 0.6
I	8.1 ± 0.5	8.3 ± 0.6	7.7 ± 0.2	7.1 ± 0.4	7.2 ± 0.3	6.5 ± 0.5	–
II	15.6 ± 1.4	15.1 ± 1.2	13.8 ± 0.9	14.8 ± 0.9	15.3 ± 1.1	12.5 ± 1.1	14.5 ± 0.5
Parasubiculum total	3.5 ± 0.2	4.0 ± 0.4	3.4 ± 0.2	3.8 ± 0.3	4.0 ± 0.2	3.9 ± 0.2	3.8 ± 0.1
I	0.9 ± 0.1	1.2 ± 0.1	1.0 ± 0.1	1.1 ± 0.04	1.1 ± 0.1	1.1 ± 0.03	1.1 ± 0.04
II	2.6 ± 0.2	2.8 ± 0.2	2.4 ± 0.2	2.7 ± 0.2	2.9 ± 0.2	2.8 ± 0.1	2.7 ± 0.1

[1]N = 4 per age (2 males, 2 females); average across ages: n = 24 individuals (12 males, 12 females). Note that an average value was calculated only when there was no statistical difference between age groups.

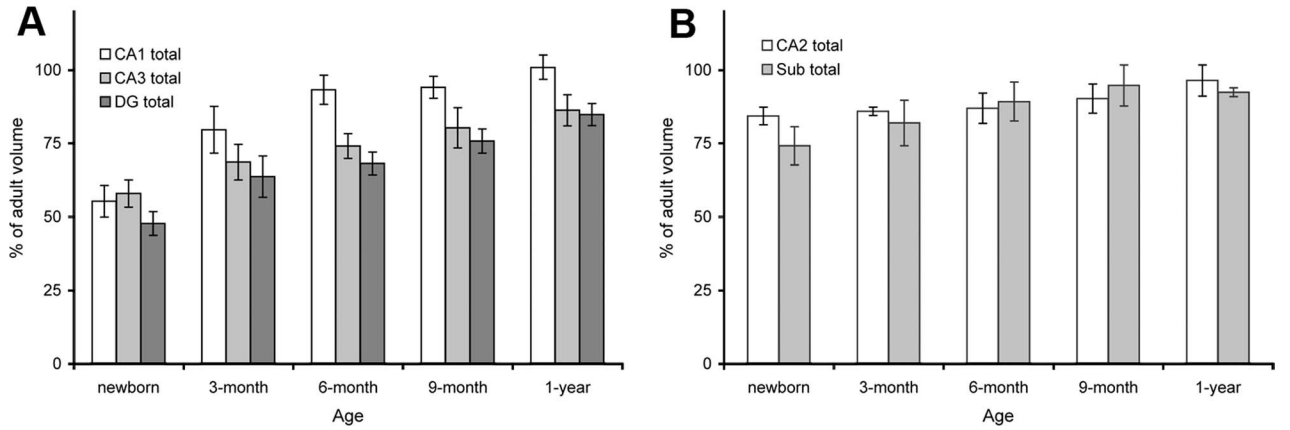

Figure 3. Volume of distinct regions of the monkey hippocampal formation at different ages during early postnatal development (expressed as percentage of the volume of the structure observed in 5–9-year-old monkeys: average ± SEM). **A**: Dentate gyrus, CA3 and CA1. **B**: CA2 and subiculum.

volume of the molecular layer also differed between age groups ($F_{5,18} = 17.105$, $P < 0.001$) and exhibited a developmental profile relatively similar to that of the granule cell layer. In newborn monkeys, the volume of the molecular layer was only 43% of that observed in 5–9-year-old monkeys; in 1-year-olds, it was 85% of the volume observed in 5–9-year-olds. The volume of the polymorphic layer exhibited a different developmental profile. Although the volume of the polymorphic layer also differed between age groups ($F_{5,18} = 11.267$, $P < 0.001$), it exhibited only a marginal difference between newborn (56% of 5–9-year-old size) and 9-month-old monkeys (67% of 5–9-year-old size). In contrast, it exhibited a significant growth past 9 months and 1 year of age (80% of 5–9-year-old size) to reach the volume observed at 5–9 years of age (5–9 years > all, $P < 0.05$; 1 year > newborn, 3 months, 6 months; $P < 0.05$).

Comparison of the percentage of the adult volume for the three layers of the dentate gyrus within the first postnatal year confirmed that these layers exhibited different developmental profiles (Fig. 4A; layers: $F_{2,30} = 49.951$, $P < 0.001$; ages: $F_{4,30} = 5.534$, $P = 0.006$; interaction $F_{8,30} = 6.476$, $P < 0.001$). At birth, the molecular layer was relatively less developed than the granule cell and polymorphic layers (both $P < 0.001$), but it had the same developmental level as the granule cell layer by 1 year of age ($P = 0.302$). In contrast, the volumetric development of the polymorphic layer was lower than that of the other two layers at 1 year of age (both $P < 0.05$). These data suggest that distinct, putative functional circuits within the dentate gyrus exhibit different developmental profiles.

CA3

We distinguished two subregions: proximal and distal CA3. Proximal CA3 occupies much of the region enclosed within the limbs of the dentate gyrus; it is not composed of clearly defined layers and does not appear to receive direct inputs from the entorhinal cortex (Witter and Amaral, 1991). Distal CA3 contains distinct layers (strata oriens, pyramidale, lucidum, radiatum, and lacunosum-moleculare), in which different projections terminate. In particular, the projections from entorhinal cortex layer II neurons terminate exclusively in stratum lacunosum-moleculare (Witter and Amaral, 1991). The volume of proximal CA3 differed between age groups ($F_{5,18} = 8.430$, $P < 0.001$). In newborn monkeys, the volume of proximal CA3 was only 35% of that observed in 5–9-year-old monkeys; in 1 year olds, it was 79% of the volume observed in 5–9 year olds (Fig. 4B). Similarly, the volume of distal CA3 differed between age groups ($F_{5,18} = 4.053$, $P = 0.012$). However, the volume of distal CA3 in newborn monkeys was already 68% of that observed in 5–9-year-old monkeys; in 1 year olds, it was 90% of the volume observed in 5–9-year-olds.

Comparison of their relative volumetric development between birth and 1 year of age revealed that distal CA3 was overall more mature than proximal CA3 (Fig. 4B; regions: $F_{1,15} = 53.955$, $P < 0.001$; ages: $F_{4,15} = 4.668$, $P = 0.012$; interaction: $F_{4,15} = 2.072$, $P = 0.135$). In newborn monkeys, the relative volume of proximal CA3 (35%) was much lower than that of distal CA3 (68%; $P < 0.001$). In 1-year-old monkeys, the relative size difference between proximal and distal CA3 was not statistically significant with the number of monkeys included in the study [n = 4 per age group; CA3-prox (79%), CA3-dist (90%), $P = 0.150$]. Altogether, these volumetric data suggest that distinct, putative functional circuits within subregions of CA3 exhibit different developmental profiles.

CA2

The overall volume of CA2 did not differ between age groups ($F_{5,18} = 2.014$, $P = 0.125$), and, accordingly, we

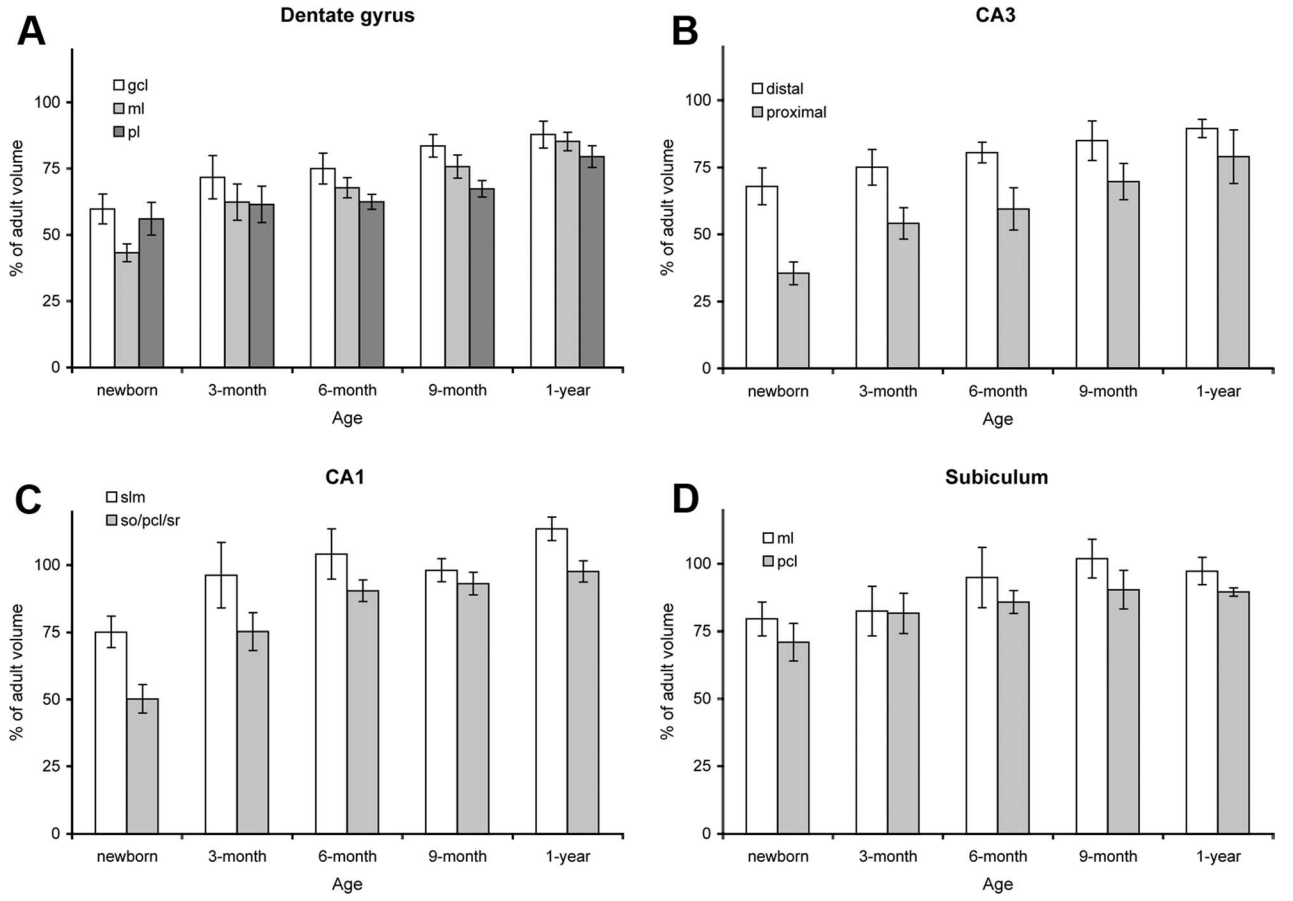

Figure 4. Volume of individual layers/regions of the monkey hippocampal formation at different ages during early postnatal development (expressed as percentage of the volume of the layer/region observed in 5–9-year-old monkeys: average ± SEM). **A**: Dentate gyrus: granule cell layer (gcl), molecular layer (ml), polymorphic layer (pl). **B**: CA3: proximal and distal portions. **C**: CA1: strata oriens, pyramidale and radiatum (so/pcl/sr), stratum lacunosum-moleculare (slm). **D**: Subiculum: stratum pyramidale (pcl), stratum moleculare (ml).

found no age differences in the volume of individual layers within CA2. Interestingly, CA2 differs from CA3 based on the absence of mossy fiber input and its interconnectivity with subcortical structures (Amaral and Lavenex, 2007). For CA2, we grouped strata oriens, pyramidale, and radiatum, which contain the CA3/CA2 associational connections and found no age differences ($F_{5,18} = 1.724$, $P = 0.180$). Similarly, the volume of CA2 stratum lacunosum-moleculare, in which entorhinal cortex projections terminate, did not differ among age groups ($F_{5,18} = 0.971$, $P = 0.461$). These volumetric data suggest that CA2, and at least some of its functional circuits, exhibit an early maturation.

CA1

We grouped strata oriens, pyramidale, and radiatum (CA1-so/pcl/sr), which contain the projections from CA3 (Schaffer collaterals), and considered stratum lacunosum-moleculare (CA1-slm), in which the entorhinal cortex projections terminate, separately (Amaral and Lavenex, 2007). The volume of CA1-so/pcl/sr differed between age groups ($F_{5,18} = 14.316$, $P < 0.001$); in newborn monkeys, it was 50% of the size observed in mature 5–9-year-old monkeys; in 6-month-olds, it was 90% of the mature size (newborn < all other ages, $P < 0.05$; 3 months < all other ages, $P < 0.05$). In contrast, age differences in the volume of CA1-slm failed to reach significance with four animals per age group ($F_{5,18} = 2.517$, $P = 0.068$). Nevertheless, the volume of CA1-slm did not appear to be adult-like in newborn monkeys (75% of 5–9-year-old size) but was 96% of its mature volume in 3-month-old monkeys.

Comparison of their relative volumetric development between birth and 1 year of age revealed that CA1-slm was overall more developed than CA1-so/pcl/sr (Fig. 4C; layers: $F_{1,15} = 62.727$, $P < 0.001$; ages $F_{4,15} = 7.065$, $P = 0.002$; interaction: $F_{4,15} = 2.816$, $P = 0.063$). In newborn monkeys, the relative volume of CA1-so/pcl/sr (50%) was lower than that of CA1-slm (75%; $P < 0.001$). In 9-month-old monkeys, the difference in the relative volume of both layers was not significant [CA1-so/pcl/sr (93%), CA1-slm (98%), $P = 0.294$]. These volumetric data

suggest that distinct, putative functional circuits within CA1 exhibit different developmental profiles.

Subiculum

We distinguished stratum pyramidale (Sub-pcl), in which most projections from CA1 terminate, and the molecular layer (Sub-ml), in which both some CA1 projections and the entorhinal cortex projections terminate (Amaral and Lavenex, 2007). The volume of Sub-pcl differed between age groups ($F_{5,18} = 2.962$, $P = 0.040$). In newborn monkeys, the volume of Sub-pcl was 71% of that observed in 5–9-year-old monkeys; in 1-year-olds, it was 90% of the mature volume. In contrast, the volume of Sub-ml did not differ significantly between age groups with four animals per age group ($F_{5,18} = 1.513$, $P = 0.235$). Nevertheless, the volume of Sub-ml was only 80% of 5–9-year-old size in newborn monkeys and 97% in 1-year-olds.

Comparison of their relative volumetric development between birth and 1 year of age indicated that the molecular layer was overall more developed than the pyramidal cell layer (layers: $F_{1,15} = 10.302$, $P < 0.006$; ages: $F_{4,15} = 1.733$, $P = 0.195$; interaction: $F_{4,15} = 0.590$, $P = 0.675$). At each age, however, the difference in the relative volume of both layers failed to reach significance with the number of monkeys included in the study ($n = 4$ per age group). Nevertheless, these volumetric data suggest that distinct, putative functional circuits within the subiculum exhibit different developmental profiles.

Presubiculum

The volume of layer I differed between age groups ($F_{5,18} = 2.837$, $P = 0.046$). In newborn monkeys, the volume of layer I was surprisingly larger than that observed in 5–9-year-old monkeys (125%); in 1-year-olds, it was 111% of its mature size. In contrast, the volume of layer II did not differ between age groups ($F_{5,18} = 1.118$, $P = 0.386$) with four animals per age group. Nevertheless, the volume of layer II was similarly, respectively, 125% and 123% in newborn and 1-year-old monkeys compared with 5–9-year-olds. Comparison of their relative volumetric development within the first year of postnatal life confirmed that the two layers of the presubiculum did not have different profiles of postnatal development (layers: $F_{1,15} = 0.202$, $P < 0.659$; ages: $F_{4,15} = 0.709$, $P = 0.598$; interaction: $F_{4,15} = 1.322$, $P = 0.307$). These volumetric data suggest a distinctive, regressive maturational process of the presubiculum.

Parasubiculum

We found no age-related differences in the volumes of layer I ($F_{5,18} = 1.505$, $P = 0.238$) or layer II ($F_{5,18} = 0.724$, $P = 0.614$) of the parasubiculum. These volumetric data suggest that the parasubiculum exhibits an early maturation compared with other hippocampal regions.

DISCUSSION

This stereological analysis of Nissl-stained coronal brain sections demonstrates that the macaque monkey hippocampal formation is far from mature at birth and that distinct hippocampal regions and layers exhibit different profiles of structural development during early postnatal life. We first discuss the contribution of our quantitative findings to the overall understanding of the structural, postnatal development of the primate hippocampal formation. We then discuss the functional implications of the differential development of distinct hippocampal circuits for the emergence and maturation of different types of "hippocampus-dependent" memory processes.

Neuron number

Our quantitative evaluation of neuron number in the different regions of the rhesus monkey hippocampal formation extends the results of a previous study (Keuker et al., 2003) and provides a comprehensive, reliable reference regarding neuron numbers in the macaque monkey hippocampal formation. We found that neurogenesis in the dentate gyrus occurs at a relatively high rate within the monkeys' first postnatal year (Jabès et al., 2010), impacting granule cell number and therefore dentate gyrus structure for a longer developmental period than previously thought (Eckenhoff and Rakic, 1988). We also established that the number of principal neurons in the other regions of the monkey hippocampal formation is stable between birth and young adulthood (5–9 years of age). These data are consistent with earlier observations that neurogenesis ceases prenatally in these regions in monkeys (Rakic and Nowakowski, 1981), rodents (Bayer, 1980), and humans (Seress et al., 2001).

Dentate gyrus

The protracted period of neuron addition in the dentate gyrus is accompanied by a late maturation of the granule cell population, which continues beyond the first postnatal year. Consistently, the granule cell and molecular layers exhibit parallel and gradual developmental profiles during the same postnatal period, suggesting an extended development of the functional circuits to which the granule cells contribute. Previous studies reported that the dendritic length and spine density of individual granule cells increase until at least the fifth postnatal months in monkeys (Duffy and Rakic, 1983; Seress, 1992). For rats, Claiborne et al. (1990) reported no differences in total dendritic length of individual, intracellularly labeled granule cells at 35 ($n = 48$), 70 ($n = 3$ suprapyramidal cells), and 111 ($n = 2$ infrapyramidal cells) days of age. However, the number of dendritic spines per unit

length increases between 2 and 7 months of age in rats (Duffy and Teyler, 1978), which suggests a protracted postnatal development of the rat molecular layer, parallel to that observed volumetrically in monkeys (current study). Unfortunately, there are no data regarding the postnatal maturation of the afferent projections of the dentate gyrus in rodents or primates. Although it has been shown that entorhinal and subcortical projections innervate the dentate gyrus during fetal development in both species (Frotscher and Seress, 2007), no study has evaluated the possible postnatal maturation of the entorhinal projections in rats or monkeys. Only one study revealed an increase in ChAT immunoreactivity (reflecting subcortical cholinergic innervation) between P16 and P32 in rats (Aznavour et al., 2005). Similarly, we published preliminary findings showing that entorhinal fibers innervate the appropriate target zones in the dentate gyrus and hippocampus of 3-week-old monkeys (Lavenex et al., 2007a), but we have yet to perform quantitative analyses of these projections in both infant and adult monkeys in order to evaluate their possible postnatal maturation. In humans, there is to our knowledge no information regarding the developmental stage of entorhinal-dentate gyrus projections at birth. Nevertheless, the myelination of these projections appears to occur largely during the postnatal period and is thought to continue even past the first decade of life in humans (Abraham et al., 2010). Altogether, these data suggest that, although the main afferent connections of the dentate gyrus are already present at birth in primates, they undergo important morphological maturation during postnatal life that might impact the functional properties of these pathways. Moreover, the maturation of subcortical projections and associational projections originating in the polymorphic layer of the dentate gyrus (see below) might also contribute to some of the volumetric changes observed in the molecular layer.

With respect to the late maturation of the granule cells, we might expect that their axons continue to mature and influence the development of their target cells in the polymorphic layer of the dentate gyrus and the CA3 field of the hippocampus during postnatal life. Indeed, we showed that the polymorphic layer exhibits an increase in volume beyond the first year of life, suggesting a protracted maturation of its cellular components. It has been reported that the mossy cells, the major targets of the granule cell projections in the polymorphic layer (Amaral, 1978; Buckmaster and Amaral, 2001), exhibit clear morphological changes in soma and dendritic structure until at least 9 months of age in monkeys (qualitative data; Seress and Ribak, 1995a) and at least 30 months of age in humans (qualitative data; Seress and Mrzljak, 1992). In addition, the number of spines per 100 μm of dendrite appears to increase by about 10% between 1 year and 4–20 years of age in monkeys (Seress and Ribak, 1995a). Our analyses revealed a 25% increase in volume of the polymorphic layer between 1 year and 5–9 years of age. Although the mossy cells and the axons of granule cells represent a major component of the polymorphic layer, a variety of other neuronal types and afferent projections target this area (Amaral and Lavenex, 2007; Amaral et al., 2007). Despite the early establishment of subcortical projections to the polymorphic layer of the dentate gyrus, myelination happens relatively late in the polymorphic layer, compared with other hippocampal regions, in humans (Abraham et al., 2010). In sum, the postnatal development of the polymorphic layer circuits is likely delayed compared with that of the dentate gyrus afferents reaching the molecular layer. However, detailed analyses of the postnatal maturation of the different cell types contained in the dentate gyrus will be necessary to provide a definite answer regarding the functional consequences of this delayed maturation.

CA3

The developmental increase in volume of CA3 generally parallels that of the dentate gyrus. However, the distal portion of CA3, which receives direct projections from layer II neurons of the entorhinal cortex, matures volumetrically earlier than the proximal portion of CA3 (Fig. 4B). We found at the cellular level that the proximal CA3 pyramidal neurons exhibit significant changes in soma size within the first 3–6 postnatal months. In contrast, the size of distal CA3 pyramidal neurons did not vary during postnatal development. Our quantitative data are thus in agreement with the qualitative report by Seress and Ribak (1995b) showing that the somas and dendrites of distal CA3 pyramidal neurons exhibit adult-like ultrastructural features at birth. There is, unfortunately, no published information on the ultrastructural characteristics of developing proximal CA3 pyramidal neurons.

Functionally, proximal and distal CA3 pyramidal neurons might contribute to different hippocampal circuits. Indeed, proximal CA3 pyramidal cells typically display no or very few dendrites extending into stratum lacunosum-moleculare in 33–57-day-old rats (Ishizuka et al., 1995) or 10-month-old to 21-year-old monkeys (Buckmaster and Amaral, 2001) and are therefore not in a position to receive significant, direct inputs from the entorhinal cortex (Witter and Amaral, 1991). In contrast, pyramidal neurons located in the proximal portion of CA3 receive large numbers of mossy fiber terminals on their apical and basal dendrites and are thus under greater influence of the granule cells than distally located CA3 cells that receive only apical mossy fiber inputs (Amaral and Lavenex, 2007; Kondo et al., 2008). As mentioned above,

various aspects of the dentate gyrus structure mature late during postnatal development; this is also the case for the mossy fiber projections. Indeed, Timm-stained mossy fiber terminals, although visible at birth, become more heavily stained in 3-month-old and adult monkeys (Seress and Ribak, 1995b). Moreover, the width of CA3 stratum lucidum (in which the mossy fibers travel and terminate) increases further after 6 months of age (see Seress and Ribak, 1995b). Our own measurements of the volume of the end bulb (the zone of stratum lucidum located distally in CA3, where the mossy fibers bend rostrally and travel longitudinally; Kondo et al., 2008) also revealed a continued increase in size between 9 months and 1 year of age. Consequently, the earlier structural maturation of distal CA3 pyramidal neurons, compared with proximal CA3 pyramidal neurons, suggests a differential maturation of distinct, putative functional circuits within CA3: a relatively early-maturing system associated with the entorhinal cortex projections (see also below for CA1 and the subiculum) and a rather late-maturing system associated with the mossy fiber projections of the dentate granule cells.

CA1

Developmental changes in volume reveal that CA1 matures relatively earlier than the dentate gyrus and CA3, despite the fact that CA3 pyramidal neurons contribute the largest projection to CA1 pyramidal neurons via the so-called Schaffer collaterals (Amaral and Lavenex, 2007; Kondo et al., 2009). CA1 stratum lacunosum-moleculare, in which the projections from the entorhinal cortex layer III neurons terminate, matures earlier than CA1 strata oriens, pyramidale, and radiatum, in which the CA3 projections terminate. Our quantitative measurements are in agreement with recent qualitative reports of a later myelination of fibers in strata pyramidale and radiatum, compared with stratum lacunosum-moleculare, in CA1 of humans (Abraham et al., 2010). In rats, the basal dendrites in stratum oriens and the terminal dendrites in stratum lacunosum-moleculare develop first (Pokorny and Yamamoto, 1981a). Specifically, the length and number of dendritic segments reach adult values as early as postnatal day 10 in CA1 stratum lacunosum-moleculare, whereas they continue to develop until postnatal day 48 in CA1 stratum radiatum. Similarly, the maturation of axon terminals, spines, and synapses takes place earlier in CA1 stratum lacunosum-moleculare than in stratum radiatum [N.B.: beware of the different nomenclature used in the original publication by Pokorny and Yamamoto (1981b)]. Altogether these data suggest a differential maturation of distinct, putative functional circuits within CA1: a relatively early-maturing system associated with the entorhinal cortex projections reaching stratum lacunosum-moleculare (see also above for CA3 and below for the subiculum) and a rather late-maturing system associated with the Schaffer collateral projections from CA3.

Subiculum and CA2

Developmental changes in volume indicated that the subiculum was more mature than CA1 until 6 months of age. However, similar to what was observed in CA1, the molecular layer of the subiculum, in which the projections from entorhinal cortex layer III neurons terminate, was overall more mature within the first postnatal year compared with the stratum pyramidale, in which most of the CA1 projections terminate. Unfortunately, there are no published data on the postnatal maturation of the different layers of the subiculum in primates or any other species. Our quantitative data therefore suggest a differential maturation of distinct, putative functional circuits within the subiculum: a relatively early-maturing system associated with the entorhinal cortex projections and a rather late-maturing system associated with the CA1 projections.

In addition, our quantitative volumetric measurements revealed that the subiculum develops earlier than the dentate gyrus, CA3, and CA1, but not CA2. These data are consistent with our preliminary observations based on the immunohistochemical detection of nonphosphorylated high-molecular-weight neurofilaments, which revealed an early maturation of the subiculum and CA2 (Lavenex et al., 2004). These two structures differ from the dentate gyrus, CA3, and CA1 based on their particular connections with subcortical structures (Amaral and Lavenex, 2007). The subiculum is one of the two primary output structures of the hippocampal formation (the entorhinal cortex being the other; Amaral and Lavenex, 2007) and is the major source of efferent projections toward subcortical structures (Naber and Witter, 1998; Swanson and Cowan, 1975). The most prominent subcortical projections of the subiculum reach the lateral septal nuclei, the nucleus accumbens, and the mammillary nuclei. In contrast, CA2 projects extensively to the hippocampus proper (CA3, CA2, and CA1), has no known projections toward the neocortex, and does not project extensively to subcortical structures. However, CA2 receives a particularly prominent innervation from the posterior hypothalamus, especially from the supramammillary area and the tuberomammillary nucleus (Amaral and Lavenex, 2007). These projections terminate mainly in and around the pyramidal cell layer and mainly on principal cells, a region that exhibits early expression of nonphosphorylated high-molecular-weight neurofilament immunoreactivity (Lavenex et al., 2004). CA2 pyramidal neurons are also more strongly excited by entorhinal

cortex inputs onto their distal dendrites in stratum lacunosum-moleculare compared with CA3 and CA1 pyramidal neurons (Chevaleyre and Siegelbaum, 2010). CA2 neurons, in turn, make strong excitatory synaptic contacts with CA1 neurons and could contribute, together with direct inputs from entorhinal cortex layer III neurons to the CA1 stratum lacunosum-moleculare, to the firing of CA1 pyramidal neurons in the absence of excitatory inputs from CA3 pyramidal neurons. Altogether, these data suggest how the subiculum, CA2, and CA1 might mature both structurally and functionally earlier than their main source of excitatory inputs in the adult hippocampal formation.

Presubiculum and parasubiculum

The volumetric developmental profile of the presubiculum was unique. Unlike all of the other hippocampal fields, there was evidence here for regressive events in the structural maturation of presubicular neurons and circuits (i.e., decrease in neuronal soma size and volume of layer I between birth and 5–9 years of age). We do not know, however, what specific cellular changes could contribute to this particular maturational profile. Our volumetric measurements also suggest an early maturation of the parasubicular circuits compared with the rest of the hippocampal formation. Two unique features of these structures, compared with other hippocampal regions, are their reciprocal connections with the anterior thalamic nuclear complex and their heavy cholinergic innervation. It is interesting to note that both the presubiculum and the parasubiculum also receive direct inputs from the retrosplenial cortex and give rise to a direct, albeit minor, projection to the molecular layer of the dentate gyrus. Functionally, experiments in rats have shown that the presubiculum contains so-called head-direction cells, whereas some neurons in the parasubiculum discharge in relation to the rat's location in the environment, so-called place cells, which are found primarily in the hippocampus proper (O'Keefe, 2007; Taube, 1995). Accordingly, cells in the presubiculum and parasubiculum might contribute to the elaboration of a primitive spatial representation of the environment before the other hippocampal circuits become functional (Langston et al., 2010). The exact nature of this representation remains to be determined.

Functional implications

The hippocampal formation, as a whole functional unit (Amaral and Lavenex, 2007; Lavenex and Amaral, 2000), is essential for the processing of declarative memory, which includes the representations of unique personal experiences called episodic memories (Squire and Zola, 1996). In humans, significant changes in the capacity for declarative memory occur within the first 4–5 years of life (Bauer, 2006; Richmond and Nelson, 2007), but the neurobiological basis for such changes has remained highly hypothetical because of the lack of systematic, quantitative studies of hippocampal development at the cellular or systems level (Bauer, 2006; Lavenex et al., 2007a; Payne et al., 2010; Richmond and Nelson, 2007). Our stereological data contribute to filling that void and suggest that the differential maturation of distinct hippocampal circuits (Figs. 2–4) might underlie the emergence and maturation of different memory processes, ultimately leading to the emergence of episodic memory with the maturation of all hippocampal circuits.

Spatial memory

Allocentric, spatial relational memory is the memory of our surroundings that encodes the interrelationships between individual elements that compose the environment in which we live (Banta Lavenex and Lavenex, 2009, 2010). In adult individuals, hippocampal integrity is critical for forming an allocentric representation of space that codes the goal location in relation to distant environmental cues (Banta Lavenex et al., 2006; Banta Lavenex and Lavenex, 2009; Bartsch et al., 2010; Bohbot et al., 2004; Morris et al., 1982; Nadel and Hardt, 2004; Schenk et al., 1995).

The implication of CA1 in spatial memory was prompted by the discovery of "place cells" that fire according to a rat's location in an open-field environment (O'Keefe and Dostrovsky, 1971). Much later, "grid cells" that display a grid-like pattern of firing covering the environment that a rat is exploring were found in the entorhinal cortex (Hafting et al., 2005). Consistently with the known anatomical organization of the hippocampal formation (Amaral and Lavenex, 2007; Lavenex and Amaral, 2000), lesions of the entorhinal cortex induce unstable CA1 place-cell representations of the environment (Van Cauter et al., 2008). Although CA1 receives its most prominent projection from CA3, proper functioning of CA3 is not necessary to sustain place-cell activity in CA1 (Brun et al., 2002). The fundamental characteristics of CA1 place-cell firing can therefore be mediated by direct entorhinal cortex projections to CA1 stratum lacunosum-moleculare (Brun et al., 2002) and perhaps also via entorhinal cortex projections to CA2 as suggested by a recent in vitro study of the control of CA1 pyramidal cell activity by CA2 inputs (Chevaleyre and Siegelbaum, 2010). Thus, the early maturation of direct inputs from the entorhinal cortex to CA1 (and possibly via CA2, which exhibits an even earlier maturation) might enable the elaboration of an allocentric, spatial relational representation of the environment. Indeed, we have previously shown that spatial relational memory processes are

present in 9-month-old monkeys (Lavenex and Banta Lavenex, 2006), an age at which some functional circuits within CA1, but not CA3 or the dentate gyrus, might already be mature (current study; see also Lavenex et al., 2009b, for evidence at the molecular level). In humans, the ability to utilize distal landmarks successfully to facilitate the discrimination of distinct locations in a sandbox is believed to emerge at about 21 months of age (Newcombe et al., 1998).

Other aspects of human spatial learning and memory processes emerge slightly earlier than the ability to elaborate a spatial representation of the environment that might be dependent on CA1 function. Indeed, the ability to use dead reckoning or path integration, the internal representation of external space based on the integration of sensory information self-generated during movement, is present as early as 16 months of age (Bremner et al., 1994; Newcombe et al., 1998). Interestingly, dead reckoning is dependent on the function of some hippocampal circuits, as rats with hippocampal dysfunction are impaired in using dead reckoning to navigate (Whishaw et al., 2001). Our current structural data suggest that the early structural development of the subiculum, presubiculum, and parasubiculum might contribute to the early functional maturation of "head direction cells" and "place cells" found in these structures (Langston et al., 2010; O'Keefe, 2007). Together with their reciprocal connections with the anterior thalamic nuclear complex and their direct inputs from the retrosplenial cortex, early maturation of neurons of the subicular complex might contribute to the early emergence of one type of "hippocampus-dependent" spatial memory system, dead reckoning.

Episodic memory

Episodic memory might be one of the last types of "hippocampus-dependent" memory processes to emerge, at about 3–5 years of age (Rubin, 2000). Computational models have proposed that continued neurogenesis in the adult dentate gyrus plays a fundamental role in the temporal coding of events and the formation of episodic memories (Deng et al., 2010; Weisz and Argibay, 2009). Newly generated immature neurons might contribute to increased association of events occurring close in time, whereas events occurring several days apart would be encoded separately by distinct groups of newly generated neurons that are not yet fully mature. Our current structural findings revealed a prolonged period of developmental neurogenesis and granule cell addition and a further protracted maturation of distinct dentate gyrus circuits beyond 1 year of age in monkeys. This might explain the inability to form enduring episodic memories until the dentate gyrus has become fully structurally mature. Indeed, very high levels of plasticity are typically associated with the normal development of the brain (Hensch, 2004; Knudsen, 2003), and the dentate gyrus likely is no exception. Dentate gyrus circuits, and in particular the balance between highly plastic, immature neurons and less plastic, mature neurons born earlier during development, might not be optimally tuned to contribute to the separate encoding of distinct episodes until late postnatal development.

CONCLUSIONS

Our quantitative data suggest a differential maturation of distinct functional circuits within the monkey hippocampal formation during early postnatal development. The protracted period of neuronal addition and maturation in the dentate gyrus is accompanied by the late maturation of specific layers in distinct hippocampal regions that are located downstream from the dentate gyrus within the hippocampal loop of information processing. This suggests that the developmental regulation of neurogenesis might be a limiting factor in the maturation of defined hippocampal circuits and specific memory functions. In contrast, the early maturation of defined layers in distinct hippocampal regions, which receive direct projections from the entorhinal cortex, suggests that specific circuits and certain "hippocampus-dependent" memory functions might appear earlier than others during postnatal development. Our current stereological findings are supported by our recent findings at the molecular level showing major and consistent changes in gene expression patterns between birth and 6 months of age in CA1 and between 1 year of age and young adulthood in CA3 (Lavenex et al., 2009b). In addition, other functions subserved by subcortical-hippocampal circuits might mature even earlier than those subserved by neocortical-hippocampal circuits. Primates, with their relatively slow developmental time scale, compared with rodents, might enable researchers to understand better how the structural development of distinct hippocampal circuits might contribute to the functional maturation of distinct "hippocampus-dependent" memory processes.

ACKNOWLEDGMENT

We thank the CNPRC staff, Jeff Bennett, Loïc Chareyron, Grégoire Favre, Jane Favre, Danièle Uldry, and K.C. Wells for technical assistance at various stages of the project.

LITERATURE CITED

Abraham H, Veszpremi B, Kravjak A, Kovacs K, Gomori E, Seress L. 2009. Ontogeny of calbindin immunoreactivity in the human hippocampal formation with a special emphasis on granule cells of the dentate gyrus. Int J Dev Neurosci 27: 115–127.

Abraham H, Vincze A, Jewgenow I, Veszpremi B, Kravjak A, Gomori E, Seress L. 2010. Myelination in the human hippocampal formation from midgestation to adulthood. Int J Dev Neurosci 28:401–410.

Altemus KL, Lavenex P, Ishizuka N, Amaral DG. 2005. Morphological characteristics and electrophysiological properties of CA1 pyramidal neurons in macaque monkeys. Neuroscience 136:741–756.

Amaral DG. 1978. A Golgi study of cell types in the hilar region of the hippocampus in the rat. J Comp Neurol 182: 851–914.

Amaral DG, Lavenex P. 2007. Hippocampal neuroanatomy. In: Amaral DG, Andersen P, Bliss T, Morris RGM, O'Keefe J, editor. The hippocampus book. New York: Oxford University Press. p 37–114.

Amaral DG, Insausti R, Cowan WM. 1984. The commissural connections of the monkey hippocampal formation. J Comp Neurol 224:307–336.

Amaral DG, Scharfman HE, Lavenex P. 2007. The dentate gyrus: fundamental neuroanatomical organization (dentate gyrus for dummies). Prog Brain Res 163:3–22.

Aznavour N, Watkins KC, Descarries L. 2005. Postnatal development of the cholinergic innervation in the dorsal hippocampus of rat: quantitative light and electron microscopic immunocytochemical study. J Comp Neurol 486:61–75.

Bakst I, Amaral DG. 1984. The distribution of acetylcholinesterase in the hippocampal formation of the monkey. J Comp Neurol 225:344–371.

Banta Lavenex P, Lavenex P. 2009. Spatial memory and the monkey hippocampus: not all space is created equal. Hippocampus 19:8–19.

Banta Lavenex P, Lavenex P. 2010. Spatial relational learning and memory abilities do not differ between men and women in a real-world, open-field environment. Behav Brain Res 207:125–137.

Banta Lavenex P, Amaral DG, Lavenex P. 2006. Hippocampal lesion prevents spatial relational learning in adult macaque monkeys. J Neurosci 26:4546–4558.

Bartsch T, Schonfeld R, Muller FJ, Alfke K, Leplow B, Aldenhoff J, Deuschl G, Koch JM. 2010. Focal lesions of human hippocampal CA1 neurons in transient global amnesia impair place memory. Science 328:1412–1415.

Bauer PJ. 2006. Constructing a past in infancy: a neuro-developmental account. Trends Cogn Sci 10:175–181.

Bayer SA. 1980. Development of the hippocampal region in the rat. I. Neurogenesis examined with ^{3}H-thymidine autoradiography. J Comp Neurol 190:87–114.

Bird CM, Burgess N. 2008. The hippocampus and memory: insights from spatial processing. Nat Rev Neurosci 9: 182–194.

Bohbot VD, Iaria G, Petrides M. 2004. Hippocampal function and spatial memory: evidence from functional neuroimaging in healthy participants and performance of patients with medial temporal lobe resections. Neuropsychology 18: 418–425.

Bremner JG, Knowles L, Andreasen G. 1994. Processes underlying young children's spatial orientation during movement. J Exp Child Psychol 57:355–376.

Brown MW, Aggleton JP. 2001. Recognition memory: what are the roles of the perirhinal cortex and hippocampus? Nat Rev Neurosci 2:51–61.

Brun VH, Otnass MK, Molden S, Steffenach HA, Witter MP, Moser MB, Moser EI. 2002. Place cells and place recognition maintained by direct entorhinal-hippocampal circuitry. Science 296:2243–2246.

Buckmaster PS, Amaral DG. 2001. Intracellular recording and labeling of mossy cells and proximal CA3 pyramidal cells in macaque monkeys. J Comp Neurol 430:264–281.

Chevaleyre V, Siegelbaum SA. 2010. Strong CA2 pyramidal neuron synapses define a powerful disynaptic cortico-hippocampal loop. Neuron 66:560–572.

Claiborne BJ, Amaral DG, Cowan WM. 1990. Quantitative, three-dimensional analysis of granule cell dendrites in the rat dentate gyrus. J Comp Neurol 302:206–219.

de Haas Ratzliff A, Soltesz I. 2000. Differential expression of cytoskeletal proteins in the dendrites of parvalbumin-positive interneurons vs. granule cells in the adult rat dentate gyrus. Hippocampus 10:162–168.

Deng W, Aimone JB, Gage FH. 2010. New neurons and new memories: how does adult hippocampal neurogenesis affect learning and memory? Nat Rev Neurosci 11:339–350.

Duffy CJ, Rakic P. 1983. Differentiation of granule cell dendrites in the dentate gyrus of the rhesus monkey: a quantitative Golgi study. J Comp Neurol 214:224–237.

Duffy CJ, Teyler TJ. 1978. Development of potentiation in the dentate gyrus of rat: physiology and anatomy. Brain Res Bull 3:425–430.

Eckenhoff MF, Rakic P. 1988. Nature and fate of proliferative cells in the hippocampal dentate gyrus during the life span of the rhesus monkey. J Neurosci 8:2729–2747.

Eichenbaum H, Yonelinas AP, Ranganath C. 2007. The medial temporal lobe and recognition memory. Annu Rev Neurosci 30:123–152.

Frotscher M, Seress L. 2007. Morphological development of the hippocampus. In: Amaral DG, Andersen P, Bliss T, Morris RGM, O'Keefe J, editor. The hippocampus book. New York: Oxford University Press. p115–131.

Goldstein ME, Sternberger LA, Sternberger NH. 1987. Varying degrees of phosphorylation determine microheterogeneity of the heavy neurofilament polypeptide (Nf-H). J Neuroimmunol 14:135–148.

Gould E, Reeves AJ, Fallah M, Tanapat P, Gross CG, Fuchs E. 1999. Hippocampal neurogenesis in adult Old World primates. Proc Natl Acad Sci U S A 96:5263–5267.

Gundersen HJ. 1988. The nucleator. J Microsc 151:3–21.

Gundersen HJ, Jensen EB. 1987. The efficiency of systematic sampling in stereology and its prediction. J Microsc 147: 229–263.

Hafting T, Fyhn M, Molden S, Moser MB, Moser EI. 2005. Microstructure of a spatial map in the entorhinal cortex. Nature 436:801–806.

Hensch TK. 2004. Critical period regulation. Annu Rev Neurosci 27:549–579.

Hof PR, Morrison JH. 1995. Neurofilament protein defines regional patterns of cortical organization in the macaque monkey visual system: a quantitative immunohistochemical analysis. J Comp Neurol 352:161–186.

Hornung JP, Riederer BM. 1999. Medium-sized neurofilament protein related to maturation of a subset of cortical neurons. J Comp Neurol 414:348–360.

Ishizuka N, Cowan WM, Amaral DG. 1995. A quantitative analysis of the dendritic organization of pyramidal cells in the rat hippocampus. J Comp Neurol 362:17–45.

Jabès A, Lavenex PB, Amaral DG, Lavenex P. 2010. Quantitative analysis of postnatal neurogenesis and neuron number in the macaque monkey dentate gyrus. Eur J Neurosci 31: 273–285.

Keuker JI, Luiten PG, Fuchs E. 2003. Preservation of hippocampal neuron numbers in aged rhesus monkeys. Neurobiol Aging 24:157–165.

Khazipov R, Esclapez M, Caillard O, Bernard C, Khalilov I, Tyzio R, Hirsch J, Dzhala V, Berger B, Ben-Ari Y. 2001. Early development of neuronal activity in the primate hippocampus in utero. J Neurosci 21:9770–9781.

Knierim JJ, Lee I, Hargreaves EL. 2006. Hippocampal place cells: parallel input streams, subregional processing, and

implications for episodic memory. Hippocampus 16: 755–764.
Knudsen EI. 2003. Early experience and critical periods. In: Squire LR, Bloom FE, McConnell SK, Roberts JL, Spitzer NC, Zigmond MJ, editors. Fundamental neuroscience, 2nd ed. London: Academic Press. p555–573.
Kondo H, Lavenex P, Amaral DG. 2008. Intrinsic connections of the macaque monkey hippocampal formation: I. Dentate gyrus. J Comp Neurol 511:497–520.
Kondo H, Lavenex P, Amaral DG. 2009. Intrinsic connections of the macaque monkey hippocampal formation: II. CA3 connections. J Comp Neurol 515:349–377.
Kornack DR, Rakic P. 1999. Continuation of neurogenesis in the hippocampus of the adult macaque monkey. Proc Natl Acad Sci U S A 96:5768–5773.
Langston RF, Ainge JA, Couey JJ, Canto CB, Bjerknes TL, Witter MP, Moser EI, Moser MB. 2010. Development of the spatial representation system in the rat. Science 328: 1576–1580.
Lavenex P. 2009. Neuroanatomy Methods in Humans and Animals. In: Squire LR, editor. Encyclopedia of neuroscience: Oxford: Academic Press. p269–278.
Lavenex P, Amaral DG. 2000. Hippocampal-neocortical interaction: a hierarchy of associativity. Hippocampus 10: 420–430.
Lavenex P, Banta Lavenex P. 2006. Spatial relational memory in 9-month-old macaque monkeys. Learn Mem 13:84–96.
Lavenex P, Steele MA, Jacobs LF. 2000a. Sex differences, but no seasonal variations in the hippocampus of food-caching squirrels: a stereological study. J Comp Neurol 425: 152–166.
Lavenex P, Steele MA, Jacobs LF. 2000b. The seasonal pattern of cell proliferation and neuron number in the dentate gyrus of wild adult eastern grey squirrels. Eur J Neurosci 12:643–648.
Lavenex P, Banta Lavenex P, Amaral DG. 2004. Nonphosphorylated high-molecular-weight neurofilament expression suggests early maturation of the monkey subiculum. Hippocampus 14:797–801.
Lavenex P, Banta Lavenex P, Amaral DG. 2007a. Postnatal development of the primate hippocampal formation. Dev Neurosci 29:179–192.
Lavenex P, Banta Lavenex P, Amaral DG. 2007b. Spatial relational learning persists following neonatal hippocampal lesions in macaque monkeys. Nat Neurosci 10:234–239.
Lavenex P, Banta Lavenex P, Bennett JL, Amaral DG. 2009a. Postmortem changes in the neuroanatomical characteristics of the primate brain: hippocampal formation. J Comp Neurol 512:27–51.
Lavenex P, Sugden SG, Davis RR, Gregg JP, Banta Lavenex P. 2009b. Developmental regulation of gene expression and astrocytic processes may explain selective hippocampal vulnerability. Hippocampus: DOI: 10.1002/hipo.20730.
Morris RG. 2007. Theories of hippocampal function. In: Amaral DG, Andersen P, Bliss T, Morris RGM, O'Keefe J, editor. The hippocampus book. New York: Oxford University Press. p581–713.
Morris RG, Garrud P, Rawlins JN, O'Keefe J. 1982. Place navigation impaired in rats with hippocampal lesions. Nature 297:681–683.
Naber PA, Witter MP. 1998. Subicular efferents are organized mostly as parallel projections: a double-labeling, retrograde-tracing study in the rat. J Comp Neurol 393:284–297.
Nadel L, Hardt O. 2004. The spatial brain. Neuropsychology 18:473–476.
Newcombe NS, Huttenlocher J, Bullock Drummey A, Wiley JG. 1998. The development of spatial location coding: place learning and dead reckoning in the second and third years. Cogn Dev 13:185–200.
Nowakowski RS, Rakic P. 1981. The site of origin and route and rate of migration of neurons to the hippocampal region of the rhesus monkey. J Comp Neurol 196:129–154.
O'Keefe J. 2007. Hippocampal neurophysiology in the behaving animal. In: Amaral DG, Andersen P, Bliss T, Morris RGM, O'Keefe J, editor. The hippocampus book. New York: Oxford University Press. p475–548.
O'Keefe J, Dostrovsky J. 1971. The hippocampus as a spatial map. Preliminary evidence from unit activity in the freely-moving rat. Brain Res 34:171–175.
Payne C, Machado CJ, Bliwise NG, Bachevaller J. 2010. Maturation of the hippocampal formation and amygdala in Macaca mulatta: a volumetric magnetic resonance imaging study. Hippocampus 20:922–935.
Pitkänen A, Amaral DG. 1993. Distribution of parvalbumin-immunoreactive cells and fibers in the monkey temporal lobe: the hippocampal formation. J Comp Neurol 331:37–74.
Poirier GL, Amin E, Aggleton JP. 2008. Qualitatively different hippocampal subfield engagement emerges with mastery of a spatial memory task by rats. J Neurosci 28:1034–1045.
Pokorny J, Yamamoto T. 1981a. Postnatal ontogenesis of hippocampal CA1 area in rats. I. Development of dendritic arborisation in pyramidal neurons. Brain Res Bull 7:113– 120.
Pokorny J, Yamamoto T. 1981b. Postnatal ontogenesis of hippocampal CA1 area in rats. II. Development of ultrastructure in stratum lacunosum and moleculare. Brain Res Bull 7:121–130.
Rakic P, Nowakowski RS. 1981. The time of origin of neurons in the hippocampal region of the rhesus monkey. J Comp Neurol 196:99–128.
Richmond J, Nelson CA. 2007. Accounting for change in declarative memory: a cognitive neuroscience perspective. Dev Rev 27:349–373.
Rolls ET, Kesner RP. 2006. A computational theory of hippocampal function, and empirical tests of the theory. Prog Neurobiol 79:1–48.
Rubin DC. 2000. The distribution of early childhood memories. Memory 8:265–269.
Schenk F, Grobéty M-C, Lavenex P, Lipp HP. 1995. Dissociation between basic components of spatial memory in rats. In: Alleva E, Fasolo A, Lipp H-P, Nadel L, Ricceri L, editor. Behavioural brain research in naturalistic and semi-naturalistic settings. NATO Advanced Science Institutes Series, Series D: Behavioural and social sciences. Amsterdam: Kluwer. p 277–300.
Seress L. 1992. Morphological variability and developmental aspects of monkey and human granule cells: differences between the rodent and primate dentate gyrus. Epilepsy Res Suppl 7:3–28.
Seress L. 2001. Morphological changes of the human hippocampal formation from midgestation to early childhood. In: Nelson CA, Luciana M, editors. Handbook of developmental cognitive neuroscience. Cambridge, MA: The MIT Press. p45–58.
Seress L, Mrzljak L. 1992. Postnatal development of mossy cells in the human dentate gyrus: a light microscopic Golgi study. Hippocampus 2:127–141.
Seress L, Ribak CE. 1995a. Postnatal development and synaptic connections of hilar mossy cells in the hippocampal dentate gyrus of rhesus monkeys. J Comp Neurol 355:93–110.
Seress L, Ribak CE. 1995b. Postnatal development of CA3 pyramidal neurons and their afferents in the Ammon's horn of rhesus monkeys. Hippocampus 5:217–231.
Seress L, Abraham H, Tornoczky T, Kosztolanyi G. 2001. Cell formation in the human hippocampal formation from midgestation to the late postnatal period. Neuroscience 105: 831–843.

Siegel SJ, Ginsberg SD, Hof PR, Foote SL, Young WG, Kraemer GW, McKinney WT, Morrison JH. 1993. Effects of social deprivation in prepubescent rhesus monkeys: immunohistochemical analysis of the neurofilament protein triplet in the hippocampal formation. Brain Res 619:299– 305.

Squire LR, Zola SM. 1996. Structure and function of declarative and nondeclarative memory systems. Proc Natl Acad Sci U S A 93:13515–13522.

Squire LR, Wixted JT, Clark RE. 2007. Recognition memory and the medial temporal lobe: a new perspective. Nat Rev Neurosci 8:872–883.

Sternberger LA, Sternberger NH. 1983. Monoclonal antibodies distinguish phosphorylated and nonphosphorylated forms of neurofilaments in situ. Proc Natl Acad Sci U S A 80:6126–6130.

Swanson LW, Cowan WM. 1975. Hippocampo-hypothalamic connections: origin in subicular cortex, not ammon's horn. Science 189:303–304.

Taube JS. 1995. Place cells recorded in the parasubiculum of freely moving rats. Hippocampus 5:569–583.

Van Cauter T, Poucet B, Save E. 2008. Unstable CA1 place cell representation in rats with entorhinal cortex lesions. Eur J Neurosci 27:1933–1946.

Vargha-Khadem F, Gadian DG, Watkins KE, Connelly A, Van Paesschen W, Mishkin M. 1997. Differential effects of early hippocampal pathology on episodic and semantic memory. Science 277:376–380.

Weisz VI, Argibay PF. 2009. A putative role for neurogenesis in neuro-computational terms: inferences from a hippocampal model. Cognition 112:229–240.

West MJ, Gundersen HJ. 1990. Unbiased stereological estimation of the number of neurons in the human hippocampus. J Comp Neurol 296:1–22.

West MJ, Slomianka L, Gundersen HJ. 1991. Unbiased stereological estimation of the total number of neurons in thesubdivisions of the rat hippocampus using the optical fractionator. Anat Rec 231:482–497.

Whishaw IQ, Hines DJ, Wallace DG. 2001. Dead reckoning (path integration) requires the hippocampal formation: evidence from spontaneous exploration and spatial learning tasks in light (allothetic) and dark (idiothetic) tests. Behav Brain Res 127:49–69.

Witter MP, Amaral DG. 1991. Entorhinal cortex of the monkey: V. Projections to the dentate gyrus, hippocampus, and subicular complex. J Comp Neurol 307:437–459.